Synthesis and Evaluation of CC-1065 and Duocarmycin Analogs Incorporating the 1,2,3,4,11,11a-Hexahydrocyclopropa[*c*]naphtho[2,1-*b*]azepin-6-one (CNA) Alkylation Subunit: Structural Features that Govern Reactivity and Reaction Regioselectivity

Dale L. Boger* and Philip Turnbull

Department of Chemistry, The Scripps Research Institute, 10550 North Torrey Pines Road, La Jolla, California 92037

Received April 21, 1997

The synthesis of 1,2,3,4,11,11a-hexahydrocyclopropa[*c*]naphtho[2,1−*b*]azepin-6-one (CNA), a seven-membered C-ring analog of the alkylation subunits of CC-1065 and the duocarmycins, is detailed. The core structure of CNA was prepared through the implementation of an intramolecular Heck reaction for assemblage of the key tricyclic tetrahydronaphtho[2,1−*b*]azepine skeleton and a final Winstein Ar-3' spirocyclization for introduction of the reactive cyclopropane. A study of the solvolysis reactivity of *N*-BOC-CNA revealed that incorporation of the seven-membered fused C-ring system increased the reactivity 4750× compared to the corresponding five-membered C-ring analog. Solvolysis occurs with S_N2 nucleophilic attack at the more substituted carbon of the activated cyclopropane to afford exclusively the abnormal ring expansion product in a reaction that was shown to proceed with complete inversion of configuration at the reaction center. Single crystal X-ray structure analyses of *N*-CO_2Me-CNA (**29**) and CNA (**11**) and their comparisons with X-ray structures of the corresponding five- and six-membered C-ring analogs revealed the structural origins of the solvolysis regioselectivity and reactivity. The regioselectivity may be attributed to the stereoelectronic alignment of the two available cyclopropane bonds with the cyclohexadienone π-system which for **29** resides with the bond that extends to the more substituted cyclopropyl carbon. The increased reactivity may be due in part to the geometric alignment of the cyclopropane but more significantly is linked to a twist in the N^2 amide. X-ray analysis provides documentation of the disruption in the vinylogous amide stabilization as measured by a lengthening of the diagnostic C−N bond that accompanies the twist in the χ_1 dihedral angle of the N^2 amide. As the cross-conjugated vinylogous amide stabilization is diminished, the cyclopropane conjugation, bond lengths, and resulting reactivity increase. The unusual stability of the five-membered C-ring bearing alkylation subunits characteristic of the natural products is intimately linked to the extent of this vinylogous amide conjugation, and the studies support the proposal that catalysis for the DNA alkylation reaction may be due to a DNA binding-induced conformational change in the agents which serves to twist the linking N^2 amide, disrupting the vinylogous amide stabilization, and activating the agents for S_N2 nucleophilic attack.

CC-1065 (**1**)[1] and the duocarmycins **2** and **3**[2−4] are novel natural products that exhibit potent biological properties (Figure 1). The agents derive their biological activity through a characteristic DNA alkylation reaction that has been shown to proceed by a reversible adenine N3 addition to the least-substituted carbon of the activated cyclopropane at selected AT-rich sites within the minor groove.[5−14]

We have examined a series of functional analogs of the CC-1065 and duocarmycin alkylation subunits in efforts to define the fundamental relationships between structure, chemical reactivity, and the corresponding biological

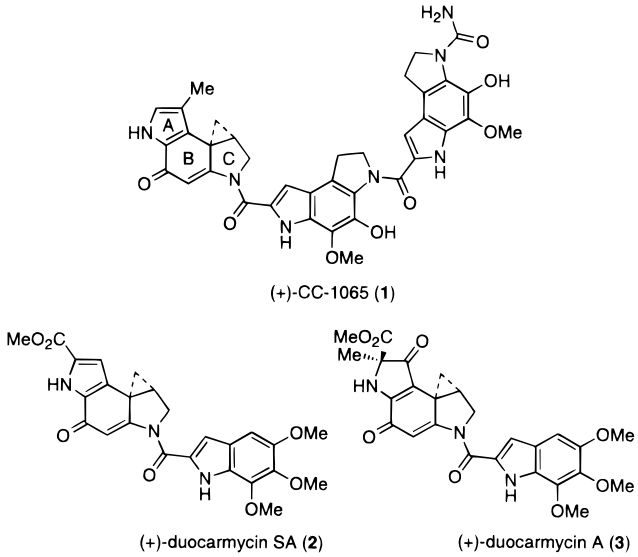

Figure 1.

⊗ Abstract published in *Advance ACS Abstracts,* August 1, 1997.

(1) Hanka, L. J.; Dietz, A.; Gerpheide, S. A.; Kuentzel, S. L.; Martin, D. G. *J. Antibiot.* **1978**, *31*, 1211. Chidester, C. G.; Krueger, W. C.; Mizsak, S. A.; Duchamp, D. J.; Martin, D. G. *J. Am. Chem. Soc.* **1981**, *103*, 7629.

(2) Yasuzawa, T.; Muroi, K.; Ichimura, M.; Takahashi, I.; Ogawa, T.; Takahashi, K.; Sano, H.; Saitoh, Y. *Chem. Pharm. Bull.* **1995**, *43*, 378. Takahashi, I.; Takahashi, K.; Ichimura, M.; Morimoto, M.; Asano, K.; Kawamoto, I.; Tomita, F.; Nakano, H. *J. Antibiot.* **1988**, *41*, 1915. Yasuzawa, T.; Iida, T.; Muroi, K.; Ichimura, M.; Takahashi, K.; Sano, H. *Chem. Pharm. Bull.* **1988**, *36*, 3728. Ichimura, M.; Muroi, K.; Asano, K.; Kawamoto, I.; Tomita, F.; Morimoto, M.; Nakano, H. *J. Antibiot.* **1988**, *41*, 1285.

(3) Ichimura, M.; Ogawa, T.; Takahashi, K.; Kobayashi, E.; Kawamoto, I.; Yasuzawa, T.; Takahashi, I.; Nakano. H. *J. Antibiot.* **1990**, *43*, 1037. Ichimura, M.; Ogawa, T.; Katsumata, S.; Takahashi, K.; Takahashi, I.; Nakano. H. *J. Antibiot.* **1991**, *44*, 1045.

(4) Ohba, K.; Watabe, H.; Sasaki, T.; Takeuchi, Y.; Kodama, Y.; Nakazawa, T.; Yamamoto, H.; Shomura, T.; Sezaki, M.; Kondo, S. *J. Antibiot.* **1988**, *41*, 1515. Ishii, S.; Nagasawa, M.; Kariya, Y.; Yamamoto, H.; Inouye, S.; Kondo, S. *J. Antibiot.* **1989**, *42*, 1713.

S0022-3263(97)00708-1 CCC: $14.00

properties.[5] Replacing the A-ring pyrrole found in **4**−**6** with a phenyl group allowed for the simplified synthesis[15] of a variety of modified alkylation subunits (Figure 2). Our first example of such a simplified derivative in this series, CBI (**8**), demonstrated remarkable biological and chemical properties.[16] In addition to being 4× more stable than CC-1065 and related CPI-derived agents, it proved considerably more regioselective in its reaction with nucleophiles. Derivatization of CBI with the appropriate DNA binding subunits gave agents that are 4× more potent than (+)-CC-1065, and selected agents within this series have exhibited efficacious antitumor activity.[17] The ring expansion of the fused five-membered C-ring found in CBI to a six-membered ring with CBQ (**9**) resulted in a substantial increase in solvolytic reactivity, a loss of the characteristic solvolysis regioselectivity, and a corresponding loss in cytotoxic potency.[18] Herein, we detail the extension of these studies to the synthesis and examination of 1,2,3,4,11,11a-hexahydrocyclopropa[*c*]naphtho[2,1−*b*]azepin-6-one (CNA, **11**), a fused seven-membered C-ring analog, and its comparison with prior agents.

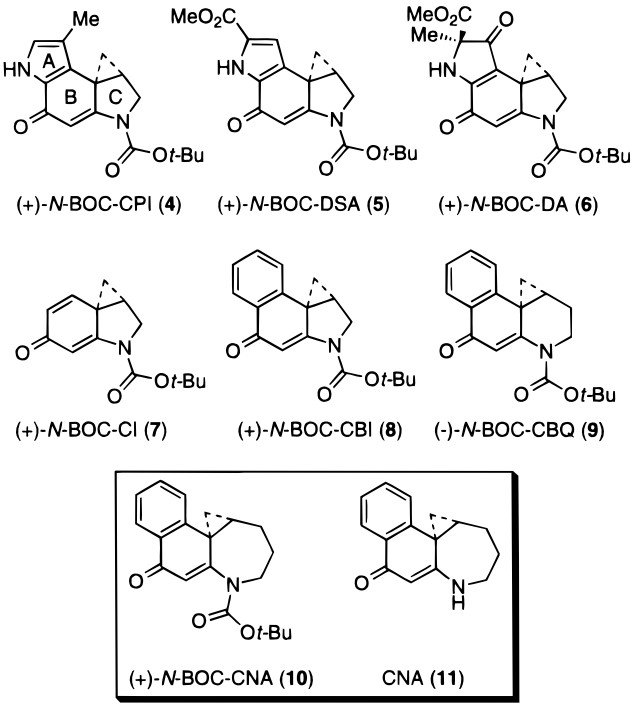

Figure 2.

Synthesis of *N*-BOC-CNA (10) and CNA (11). Attempts to extend the radical cyclization methodology employed for the five- and six-membered C-ring analogs in this class were unsuccessful.[16−19] Reaction of the appropriately functionalized naphthalene[20] with Bu_3SnH−AIBN (R = H, + TEMPO) resulted in simple reduction (eq 1). The metal hydride reduction of the resulting aryl radical proved faster than the required 7−*exo*-*trig* radical cyclization even with substrates bearing an activated acceptor alkene.

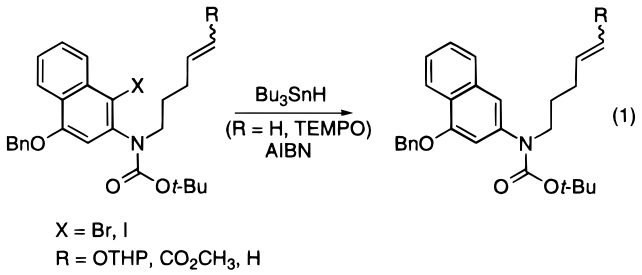

(5) Boger, D. L.; Johnson, D. S. *Angew. Chem., Int. Ed. Engl.* **1996**, *35*, 1439. Boger, D. L.; Johnson, D. S. *Proc. Natl. Acad. Sci. U.S.A.* **1995**, *92*, 3642. Boger, D. L. *Acc. Chem. Res.* **1995**, *28*, 20. Boger, D. L. *Chemtracts: Org. Chem.* **1991**, *4*, 329. Boger, D. L. *Proc. Robert A. Welch Found. Conf. Chem. Res., XXXV. Chem. Front. Med.* **1991**, *35*, 137. Boger, D. L. In *Advances in Heterocyclic Natural Products Synthesis*; Pearson, W. H., Ed.; JAI: Greenwich, CT, 1992; Vol. 2, p 1.

(6) Warpehoski, M. A.; Hurley, L. H. *Chem. Res. Toxicol.* **1988**, *1*, 315. Hurley, L. H.; Needham-VanDevanter, D. R. *Acc. Chem. Res.* **1986**, *19*, 230. Warpehoski, M. A. In *Advances in DNA Sequence Specific Agents*; Hurley, L. H., Ed.; JAI: Greenwich, CT, 1992; Vol. 1, p 217. Hurley, L. H.; Draves, P. In *Molecular Aspects of Anticancer Drug-DNA Interactions*; Neidle, S., Waring, M., Eds.; CRC: Ann Arbor, 1993; Vol. 1, p 89. Aristoff, P. A. In *Advances in Medicinal Chemistry*; JAI: Greenwich, CT, 1993; Vol. 2, p 67. Warpehoski, M. A.; McGovren, P.; Mitchell, M. A. In *Molecular Basis of Specificity in Nucleic Acid-Drug Interactions*; Pullman, B., Jortner, J., Eds.; Kluwer: Netherlands, 1990; p 531.

(7) Boger, D. L.; Ishizaki, T.; Zarrinmayeh, H.; Kitos, P. A.; Suntornwat, O. *J. Org. Chem.* **1990**, *55*, 4499. Boger, D. L.; Ishizaki, T.; Zarrinmayeh, H.; Munk, S. A.; Kitos, P. A.; Suntornwat, O. *J. Am. Chem. Soc.* **1990**, *112*, 8961. Boger, D. L.; Munk, S. A.; Zarrinmayeh, H.; Ishizaki, T.; Haught, J.; Bina, M. *Tetrahedron* **1991**, *47*, 2661. Boger, D. L.; Ishizaki, T.; Zarrinmayeh, H. *J. Am. Chem. Soc.* **1991**, *113*, 6645. Boger, D. L.; Yun, W.; Terashima, S.; Fukuda, Y.; Nakatani, K.; Kitos, P. A.; Jin, Q. *Bioorg. Med. Chem. Lett.* **1992**, *2*, 759. Boger, D. L.; Yun, W. *J. Am. Chem. Soc.* **1993**, *115*, 9872. Boger, D. L.; Johnson, D. S.; Yun, W. *J. Am. Chem. Soc.* **1994**, *116*, 1635.

(8) Boger, D. L.; Johnson, D. S. *J. Am. Chem. Soc.* **1995**, *117*, 1443. Boger, D. L.; Johnson, D. S.; Yun, W.; Tarby, C. M. *Bioorg. Med. Chem.* **1994**, *2*, 115. Boger, D. L.; Zarrinmayeh, H.; Munk, S. A.; Kitos, P. A.; Suntornwat, O. *Proc. Natl. Acad. Sci. U.S.A.* **1991**, *88*, 1431. Boger, D. L.; Munk, S. A.; Zarrinmayeh, H. *J. Am. Chem. Soc.* **1991**, *113*, 3980. Boger, D. L.; Coleman, R. S.; Invergo, B. J.; Sakya, S. M.; Ishizaki, T.; Munk, S. A.; Zarrinmayeh, H.; Kitos, P. A.; Thompson, S. C. *J. Am. Chem. Soc.* **1990**, *112*, 4623.

(9) Sugiyama, H.; Hosoda, M.; Saito, I.; Asai, A.; Saito, H. *Tetrahedron Lett.* **1990**, *31*, 7197. Sugiyama, H.; Ohmori, K.; Chan, K. L.; Hosoda, M.; Asai, A.; Saito, H.; Saito, I. *Tetrahedron Lett.* **1993**, *34*, 2179. Yamamoto, K.; Sugiyama, H.; Kawanishi, S. *Biochemistry* **1993**, *32*, 1059. Asai, A.; Nagamura, S.; Saito, H. *J. Am. Chem. Soc.* **1994**, *116*, 4171.

(10) Reynolds, V. L.; Molineux, I. J.; Kaplan, D. J.; Swenson, D. H.; Hurley, L. H. *Biochemistry* **1985**, *24*, 6228. Hurley, L. H.; Lee, C.-S.; McGovren, J. P.; Warpehoski, M. A.; Mitchell, M. A.; Kelly, R. C.; Aristoff, P. A. *Biochemistry* **1988**, *27*, 3886. Hurley, L. H.; Warpehoski, M. A.; Lee, C.-S.; McGovren, J. P.; Scahill, T. A.; Kelly, R. C.; Mitchell, M. A.; Wicnienski, N. A.; Gebhard, I.; Johnson, P. D.; Bradford, V. S. *J. Am. Chem. Soc.* **1990**, *112*, 4633.

(11) Boger, D. L.; Hertzog, D. L.; Bollinger, B.; Johnson, D. S.; Cai, H.; Goldberg, J.; Turnbull, P. *J. Am. Chem. Soc.* **1997**, *119*, 4977.

(12) Boger, D. L.; Bollinger, B.; Hertzog, D. L.; Johnson, D. S.; Cai, H.; Mesini, P.; Garbaccio, R. M.; Jin, Q.; Kitos, P. A. *J. Am. Chem. Soc.* **1997**, *119*, 4987.

(13) Boger, D. L.; Boyce, C. W.; Johnson, D. S. *Bioorg. Med. Chem. Lett.* **1997**, *7*, 233.

(14) Boger, D. L.; Johnson, D. S.; Wrasidlo, W. *Bioorg. Med. Chem. Lett.* **1994**, *4*, 631.

(15) Boger, D. L.; Boyce, C. W.; Garbaccio, R. M.; Goldberg, J. *Chem. Rev.* **1997**, *97*, 263.

(16) Boger, D. L.; Ishizaki, T.; Wysocki, R. J.; Munk, S. A.; Kitos, P. A.; Suntornwat, O. *J. Am. Chem. Soc.* **1989**, *111*, 6461. Boger, D. L.; Ishizaki, T.; Kitos, P. A.; Suntornwat, O. *J. Org. Chem.* **1990**, *55*, 5823. Boger, D. L.; Ishizaki, T. *Tetrahedron Lett.* **1990**, *31*, 793. Boger, D. L.; Ishizaki, T.; Zarrinmayeh, H.; Kitos, P. A.; Suntornwat, O. *Bioorg. Med. Chem. Lett.* **1991**, *1*, 55. Boger, D. L.; Ishizaki, T.; Sakya, S.; Munk, S. A.; Kitos, P. A.; Jin, Q.; Besterman, J. M. *Bioorg. Med. Chem. Lett.* **1991**, *1*, 115. Boger, D. L.; Munk, S. A. *J. Am. Chem. Soc.* **1992**, *114*, 5487. Boger, D. L.; Yun, W. *J. Am. Chem. Soc.* **1994**, *116*, 7996. Boger, D. L.; Yun, W.; Han, N.; Johnson, D. S. *Bioorg. Med. Chem.* **1995**, *3*, 611. Boger, D. L.; Yun, W.; Cai, H.; Han, N. *Bioorg. Med. Chem.* **1995**, *3*, 761.

(17) Boger, D. L.; Yun, W.; Han, N. *Bioorg. Med. Chem.* **1995**, *3*, 1429.

(18) Boger, D. L.; Mesini, P.; Tarby, C. M. *J. Am. Chem. Soc.* **1994**, *116*, 6461. Boger, D. L.; Mesini, P. *J. Am. Chem. Soc.* **1994**, *116*, 11335. Boger, D. L.; Mesini, P. *J. Am. Chem. Soc.* **1995**, *117*, 11647.

(19) Boger, D. L.; Yun, W.; Teegarden, B. R. *J. Org. Chem.* **1992**, *57*, 2873. Boger, D. L.; McKie, J. A. *J. Org. Chem.* **1995**, *60*, 1271.

(20) Full experimental details are provided in Supporting Information.

Scheme 1

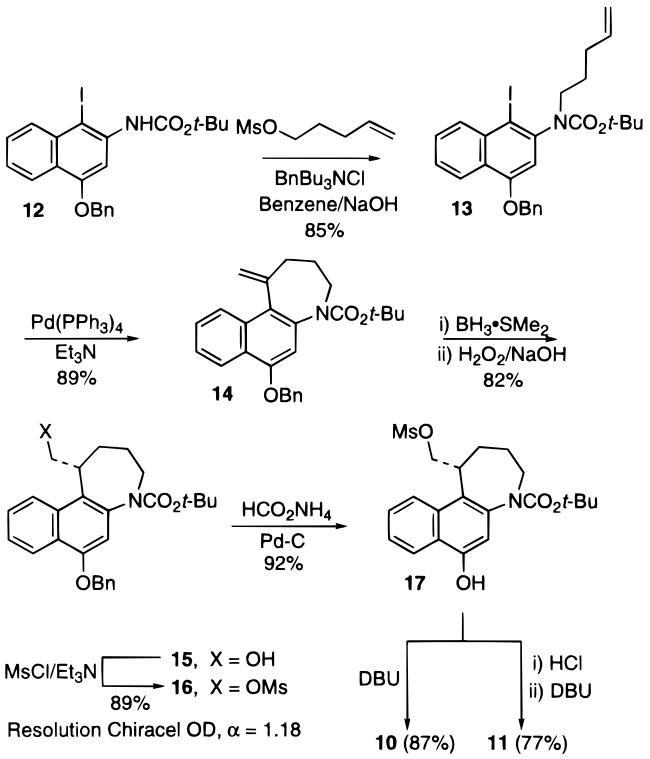

The successful approach to the preparation of the CNA nucleus rested on the implementation of an alternative intramolecular Heck reaction.[21] The starting material for both the Heck reaction and the radical cyclization attempts was prepared by *N*-alkylation of *N*-(*tert*-butyloxycarbonyl)-4−(benzyloxy)-1-iodo-2-naphthylamine (**12**), readily available in three steps (60% overall) from 1,3−dihydroxynaphthalene,[19] with the mesylate of 4-penten-1-ol to provide **13** (Scheme 1). A full 2 mol equiv of benzyltributylammonium chloride was required to provide high yields of the alkylated product using phase transfer conditions. An intramolecular Heck reaction conducted with 3 mol % of $Pd[P(Ph_3)]_4$ as catalyst furnished the desired cyclization product **14** in 89%. Careful removal of O_2 from the reaction mixture provided reproducible high yields, and no palladium hydride induced isomerization of **14** to give the endocyclic olefin was detectable by ^1H NMR of the crude reaction mixture.

Similar observations were made with the substrate (R = CO_2CH_3) bearing an activated electron-deficient acceptor alkene, but the reaction proved unsuccessful with the substrate (R = OTHP) bearing an electron-rich acceptor alkene (eq 2).[20] In principle, both successful cyclization products can be converted into appropriately C-1 substituted and functionalized tetrahydronaphtho[2,1−*b*]azepines for use in the preparation of **10** and **11**. In our efforts, **14** was employed since its conversion to **10** and **11** would follow protocols we introduced with the synthesis of CC-1065 and consequently were familiar with.[16,22]

Hydroboration followed by oxidative workup converted the exocyclic olefin into the desired alcohol **15** (82%).[16,22] Efforts to convert this alcohol to the corresponding

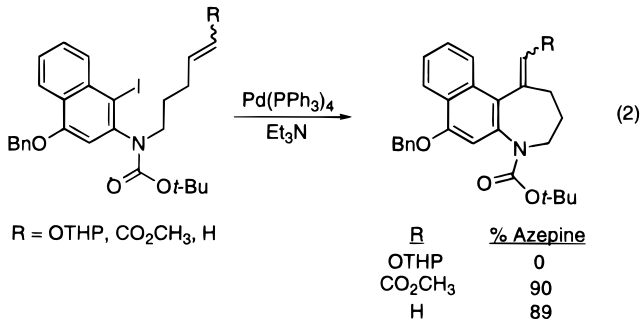

chloride **18** upon treatment with Ph_3P-CCl_4 proceeded in modest yields (*ca.* 50%, eq 3). Much higher conversions were realized by treatment of **15** with mesyl chloride in the presence of Et_3N to provide **16** in 89%. Removal of the benzyl group through transfer hydrogenolysis[23] (4 wt equiv of 10% Pd−C, aqueous HCO_2NH_4−THF, 25 °C, 2 h, 89%) afforded **17** and set the stage for the final spirocyclization.

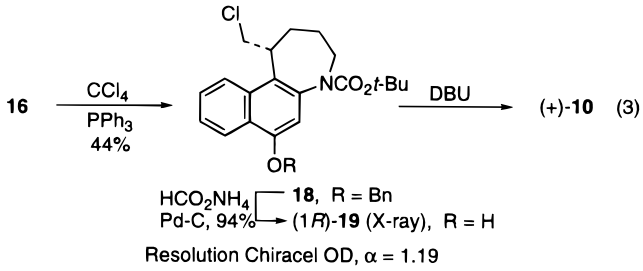

Winstein Ar-3′ spirocyclization was effected by treatment of **17** with DBU (3 equiv, CH_3CN) and smoothly provided **10** (87%). Due to its unusual reactivity, careful chromatographic conditions were required and pretreatment of the chromatographic support (SiO_2) with Et_3N resulted in much higher yields (*i.e.*, 87% versus 40−50%). Treatment of **17** with 3.9 M HCl−EtOAc removed the BOC group to afford the unstable amine hydrochloride which was taken directly into the subsequent cyclization step. Addition of 10 equiv of DBU as a dilute solution in CH_3CN resulted in good conversion to **11** (77%). Conventional chromatography provided the relatively stable CNA which gave crystals suitable for X-ray analysis[24] (CH_3CN-CH_3OH).

Synthesis of *N*-CO_2Me-CNA (29) and CNA-TMI (30). Efforts to acylate the amine hydrochloride resulting from BOC deprotection of **17** at this late stage in the synthesis were unsuccessful. The only azepine amenable to *N*-acylation was the free amine derived from **14** which bore the exocyclic olefin. Incorporation of the sp^2-hybridized carbon presumably alters the conformation of the fused seven-membered ring in a manner that allows *N*-acylation. Synthesis of the amine hydrochloride **20** through treatment with 3.9 N HCl−EtOAc (25 °C, 40 min) provided a relatively well-behaved solid amine salt that served as a short term storage intermediate for further acylations (Scheme 2). Liberation of the free amine with $NaHCO_3$ followed by treatment with methyl chloroformate provided **21** in 94% yield. High yields (80%) were also realized for EDCI coupling of **20** and

(21) Sakamoto, T.; Kondo, Y.; Uchiyama, M.; Yamanaka, H. *J. Chem. Soc., Perkin Trans. 1* **1993**, 1941. Abelman, M. M.; Oh, T.; Overman, L. E. *J. Org. Chem.* **1987**, *52*, 4130.

(22) Boger, D. L.; Coleman, R. S. *J. Am. Chem. Soc.* **1988**, *110*, 4796.

(23) Ram, S.; Ehrenkaufer, R. E. *Synthesis* **1988**, 91. Bieg, T.; Szeja, W. *Synthesis* **1985**, 76.

(24) The atomic coordinates for this structure have been deposited with the Cambridge Crystallographic Data Centre and may be obtained upon request from the Director, Cambridge Crystallographic Data Centre, 12 Union Road, Cambridge, CB2 1EZ, UK.

Scheme 2

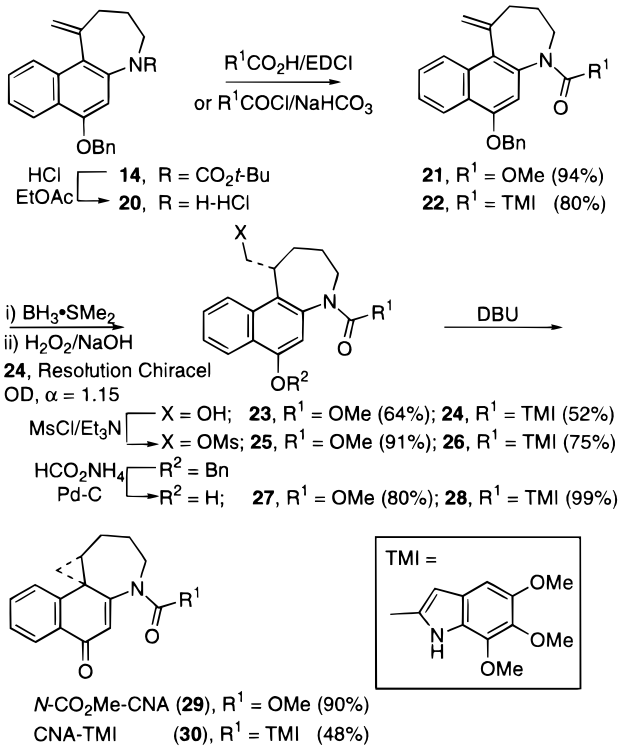

Table 1. Resolution of 16, 19, and 24[a]

agent	% *i*-PrOH−hexane, flow rate	t_R (min)	α
16	10%, 5 mL/min	38.0, 45.0	1.18
19	6%, 6 mL/min	22.6, 26.8	1.19
24	50%, 8 mL/min	14.4, 16.3	1.13
	60%, 8 mL/min	16.3, 18.5	1.13
	70%, 8 mL/min	20.9, 24.0	1.15

[a] 10 μm, 2 × 25 cm semipreparative Chiracel OD column.

5,6,7-trimethoxyindole-2-carboxylic acid to form the advanced analog **22**. Exposure of the acylated products to the same sequence of synthetic transformations detailed for **10** and **11** gave good to excellent yields of the desired products **23**−**28**. Unlike *N*-BOC-CNA (**10**), *N*-CO_2Me-CNA (**29**) proved to be a crystalline solid and recrystallization from 10% EtOAc−hexanes gave X-ray quality crystals.[24] Spirocyclization of TMI derivative **28** gave a lower yield of ring closed product **30** (48%) due to its high reactivity and more challenging chromatography requirements for purification.

Resolution. In order to obtain the separate enantiomers of both **10** and **28**, various synthetic intermediates were subjected to direct chromatographic resolution on a semipreparative chiracel OD column (Table 1). The intermediates **16**, **19**, and **24** proved to have the greatest separation and were resolved (>99.9% ee) in sufficient quantities to be carried on to the respective final products. The assignment of the absolute configuration for (+)-**10** was based initially on the relative cytotoxic potencies of (+)- and *ent*-(−)-*N*-BOC-CNA, with the former exhibiting more potent activity which is consistent with observations made for **1**-**9**. Ultimately, the absolute configuration for (+)-**10** was confirmed and unambiguously established by X-ray structure analysis[24] of the resolved *seco*-derivative (−)-(1*R*)-**19** bearing a heavy atom and subsequent conversion to (+)-**10**.

Chemical Solvolysis: Reactivity. Both the study of the rate of acid-catalyzed solvolysis and the regioselectivity of cyclopropyl ring opening have proven to be key to understanding of the structural features that dictate the properties of the duocarmycin and CC-1065 alkylation subunits.[5] Comparison of the rate of solvolysis allows for the identification of the functional features that contribute to the stabilization or activation of the cyclopropane while studies regarding the regioselectivity of the acid-catalyzed ring opening have proven key to understanding the mechanism of the DNA alkylation reaction. To date, the preferred nucleophilic addition sites appear to be dictated by the relative stereoelectronic alignment of the scissile cyclopropyl bonds with the cyclohexadienone π-system but may be influenced by the relative reactivity. Moreover, both S_N2 and S_N1 mechanisms have been advanced to account for the generation of the abnormal ring expansion solvolysis products.[11,18,25−27] In instances of mixed reaction regioselectivity, the clean generation of single DNA alkylation products derived from adenine N3 addition exclusively to the least-substituted cyclopropane carbon indicates that additional subtle features inherent in the reaction contribute to its regioselectivity.[11,18,26]

The solvolysis reactivities of *N*-BOC-CNA (**10**) and CNA (**11**) were followed spectrophotometrically by UV at both pH 3 (50% CH_3OH-buffer, buffer = 4:1:20 v/v/v 0.1 M citric acid, 0.2 M Na_2HPO_4, H_2O) and pH 7 (50% CH_3OH-H_2O), Figure 3. The reactivity of both **10** ($t_{1/2}$ = 1.7 min at pH 3) and **11** ($t_{1/2}$ = 37 min at pH 3) proved remarkable. Consistent with past observations, CNA (**11**) was considerably more stable than *N*-BOC-CNA (**10**). Unlike prior studies, both were sufficiently reactive to undergo rapid solvolysis even at pH 7. Comparison of the solvolytic reactivity of *N*-BOC-CNA with representative prior analogs reveals a reactivity that is between that of *N*-BOC-CBQ and the exceptionally reactive *N*-BOC-CI (Table 2). Particularly informative are comparisons of the benzo series of agents that differ only in the C-ring size (*i.e.*, **8**−**11**). Solvolysis reactivity smoothly increases through the series CBI < CBQ < CNA with both the *N*-BOC derivatives and the free NH derivatives. The reactivity of both *N*-BOC-CNA and CNA proved to be 4750 and 1500× more reactive than the corresponding CBI derivatives. Moreover, *N*-BOC-CNA exhibited a first-order rate constant for the solvolysis at pH 7 which is of the same order of magnitude as the characteristically rapid DNA alkylation reactions of **1**−**3**[27] without deliberate added catalysis. The agents containing the free NH, and thus the greatest degree of vinylogous amide conjugation, were 10−40× more stable to solvolysis than the corresponding *N*-BOC derivatives.[28]

Chemical Solvolysis: Regioselectivity and Mechanism. Treatment of *N*-BOC-CNA (**10**) with 0.12 equiv of CF_3SO_3H in a mixture of H_2O and THF resulted in clean solvolysis (>96%) to provide a single product (Scheme 3). No *N*-BOC deprotection or olefin formation was observed. Comparison of this single product to **33** that would result from H_2O attack at the less-substituted cyclopropyl carbon indicated that ring expansion had

(25) Boger, D. L.; Goldberg, J.; McKie, J. A. *Bioorg. Med. Chem. Lett.* **1996**, *6*, 1955.

(26) Boger, D. L.; McKie, J. A.; Nishi, T.; Ogiku, T. *J. Am. Chem. Soc.* **1997**, *119*, 311.

(27) Warpehoski, M. A.; Harper, D. E. *J. Am. Chem. Soc.* **1994**, *116*, 7573. Warpehoski, M. A.; Harper, D. E. *J. Am. Chem. Soc.* **1995**, *117*, 2951.

(28) In previous studies this rate difference was attributed to *N*- versus *O*-protonation, see: Warpehoski, M. A.; Gebhard, I.; Kelly, R. C.; Krueger, W. C.; Li, L. H.; McGovern, J. P.; Prairie, M. D.; Wicnienski, N.; Wierenga, W. *J. Med. Chem.* **1988**, *31*, 590.

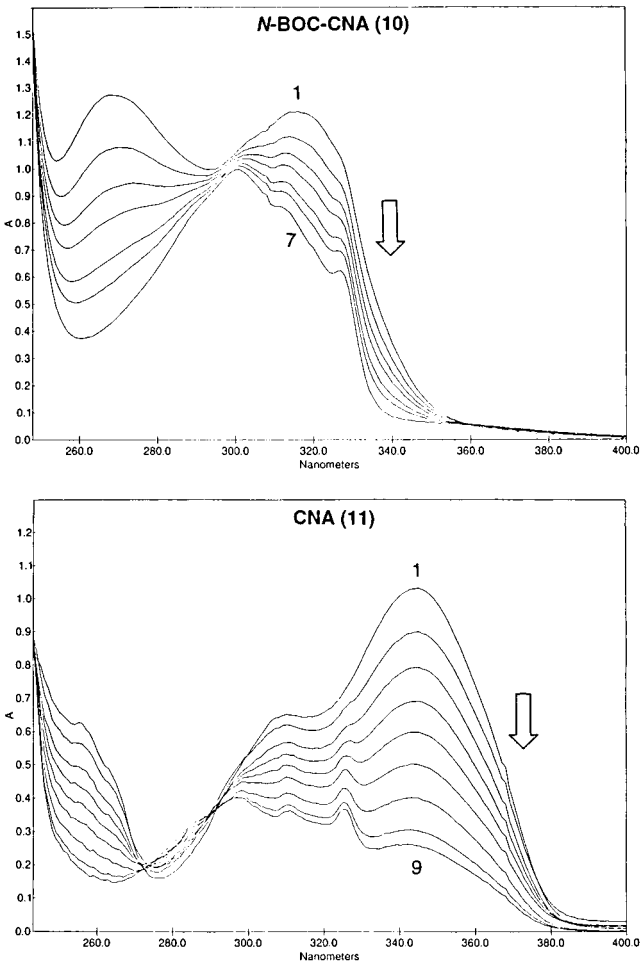

Figure 3. Solvolysis study (UV) spectra of *N*-BOC-CNA (**10**, top) and CNA (**11**, bottom) in 50% CH_3OH−aqueous buffer (pH 3.0, 4:1:20 (v/v/v) 0.1 M citric acid, 0.2 M NaH_2PO_4, and H_2O, respectively). The spectra were recorded at regular intervals, and only a few are shown for clarity. Top: 1, 0 min; 2, 0.5 min; 3, 1.0 min; 4, 1.5 min; 5, 2.5 min; 6, 3.5 min; 7, 8.5 min. Bottom: 1, 0 min; 2, 10 min; 3, 18 min; 4, 30 min; 5, 46 min; 6, 64 min; 7, 90 min; 8, 152 min; 9, 302 min.

Table 2

agent	$t_{1/2}$ (h, pH 3)	k (s^{-1}, pH 3}	$t_{1/2}$ (h, pH 7)	k (s^{-1}, pH 7)
		N-BOC Derivatives		
N-BOC-DSA (**5**)	177	1.08×10^{-6}	stable	stable
N-BOC-CPI (**4**)	37	5.26×10^{-6}	stable	stable
N-BOC-DA (**6**)	11	1.75×10^{-5}	stable	stable
N-BOC-CBI (**8**)	133	1.45×10^{-6}	stable	stable
N-BOC-CBQ (**9**)	2.1	9.07×10^{-5}	544	3.54×10^{-7}
N-BOC-CNA (**10**)	0.03	6.90×10^{-3}	2.1	9.16×10^{-5}
N-BOC-Cl (**7**)	0.01	1.98×10^{-2}	5.2	3.67×10^{-5}
		N-H Derivatives		
CBI	930	2.07×10^{-7}	stable	stable
CBQ	91.2	2.11×10^{-6}	stable	stable
CNA (**11**)	0.62	3.10×10^{-4}	563	3.42×10^{-7}

occurred exclusively to afford **31**. None of the typical seven-membered ring solvolysis product **33** could be detected in the crude reaction mixture by ^1H NMR or HPLC. Treatment of **10** with CH_3OH under similar conditions gave an analogous result, providing excellent conversion exclusively to the abnormal ring expansion product **32**. Although minor amounts of the ring expansion solvolysis products have been observed with related systems, the solvolysis of *N*-BOC-CNA represents the first observation of either predominant or exclusive ring

Scheme 3

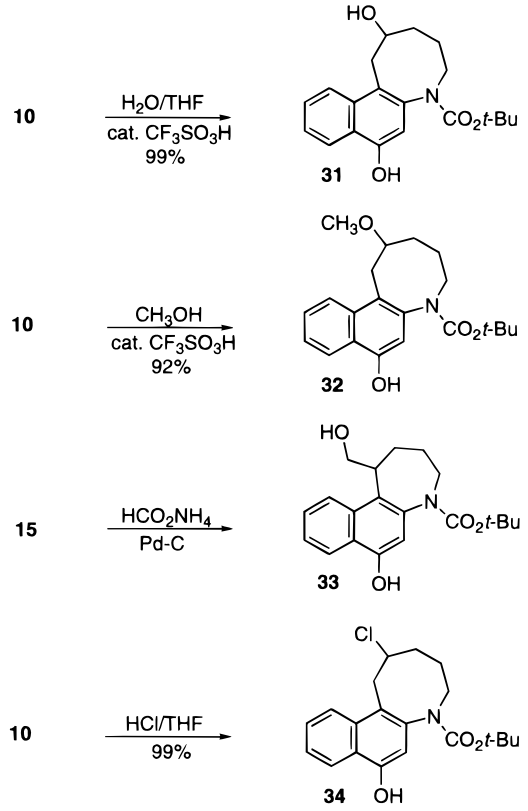

expansion derived from cleavage of the internal cyclopropane bond. Similarly, treatment of **10** with 1.5 equiv of HCl in THF (−78 °C, 15 min) cleanly provided **34** (>20:1, 99%) and not **19**. This observation is especially significant. In some,[11,27] but not all,[18,26] of the prior instances of mixed solvolysis regioselectivity, the addition of HCl still cleanly provided the typical addition product derived from attack at the least-substituted carbon rather than the ring expansion addition observed with the generation of **34**. The clean addition of HCl to **10** to provide the ring expansion product **34** illustrates that the stereoelectronic control of the addition directs even the larger nucleophiles to the more-hindered cyclopropyl carbon.

In an effort that established the mechanistic course of the reaction, both racemic and optically active (+)-**10** were subjected to acid-catalyzed solvolysis (0.12 equiv of CF_3SO_3H, H_2O−THF, 25 °C, 5 min) to provide **31**. Resolution on a Diacel Chiracel OG analytical HPLC column separated both enantiomers of the reaction product. The product derived from optically active (+)-**10** provided one enantiomer of the ring expanded product (Figure 4). The generation of a single enantiomer of **31** establishes that the cleavage of the internal cyclopropane bond does not proceed with generation of a free carbocation (S_N1) but instead occurs with clean inversion of the reaction center stereochemistry in an S_N2 ring-opening reaction. These results are in agreement with the similarly unambiguous results of solvolysis studies of *N*-BOC-CBQ,[18] *N*-BOC-DSA,[11] and *N*-BOC-DA[26] which also afford a single enantiomer of the minor ring expansion products but contrasts the studies with a CPI-derivative where racemization is reported to occur.[27] This growing set of observations and especially that of the exceptionally reactive *N*-BOC-CNA detailed herein suggest the latter CPI studies should be reexamined, em-

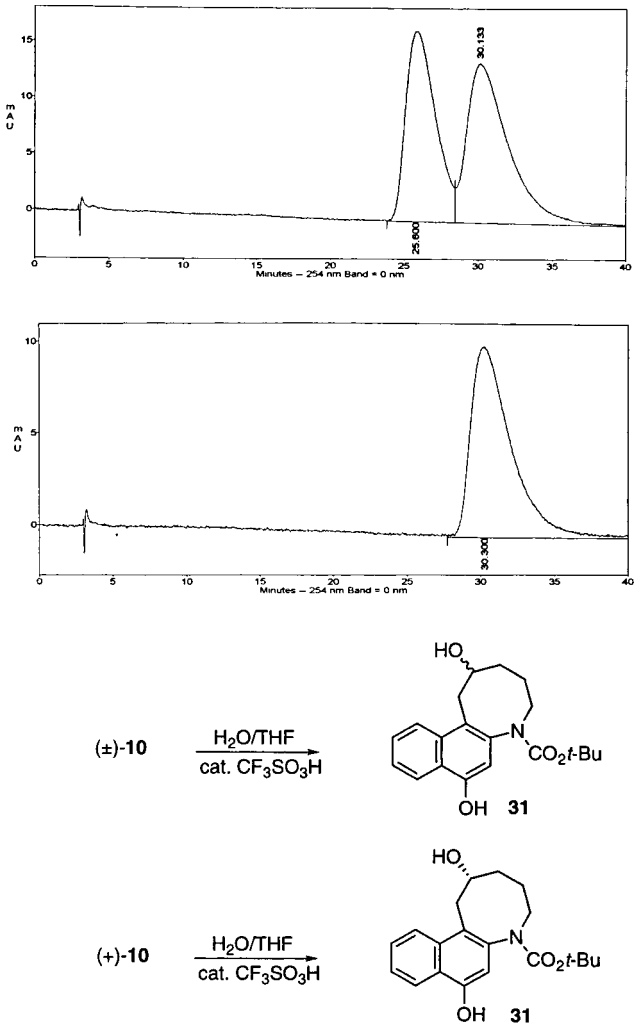

Figure 4. Chiral phase HPLC separation of the product **31** of acid-catalyzed addition of H_2O to racmic **10** (top) and (+)-**10** (bottom). Chiracel OG HPLC column (10 μm, 0.46 × 25 cm), 5% *i*-PrOH−hexane, 1 mL/min.

ploying a more definitive basis for establishing the optical purity of the ring expansion solvolysis product.

X-ray Structural Correlations with Solvolysis Regioselectivity. The single-crystal X-ray structure determination of *N*-CO_2Me-CNA (**29**) and CNA (**11**) was conducted in expectations of providing structural insights into its reversed solvolysis regioselectivity and extraordinary reactivity, Figure 5.[24] To insure the comparisons were accurately made between the appropriately acylated and nonacylated derivatives, we have also extended the efforts to secure a total of eight X-ray crystal structures[24] including both a simple *N*-acyl and the free NH derivative of CNA, CBQ, and CBI, as well as two seco precursors.

Comparison of the X-ray structures allows for a confirmation of the conclusions that have been drawn between the relative stereoelectronic alignment of the reacting cyclopropane bonds and solvolysis regioselectivity.[11,18,26,29,30] The newly obtained X-ray structure for *N*-CO_2Me-CBI containing the five-membered C-ring, like that of CBI itself,[16] reveals that the bent orbital of the cyclopropane bond extending to the least substituted

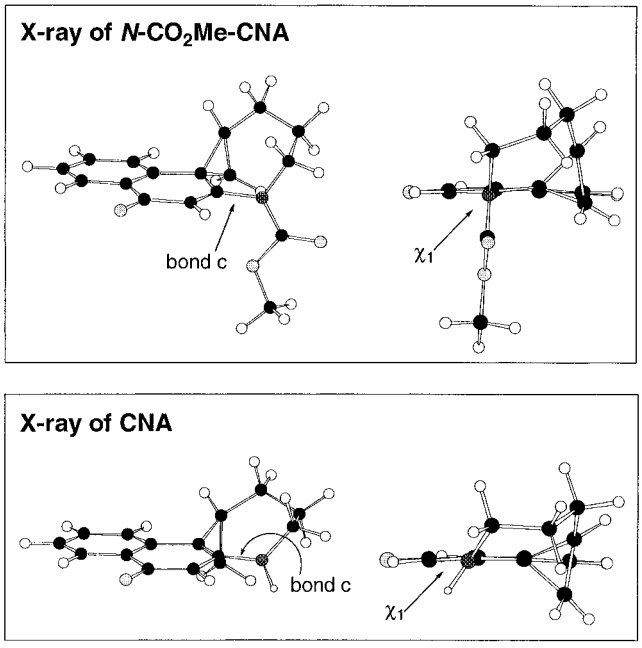

Figure 5.

carbon is nearly perpendicular to the plane of the cyclohexadienone and consequently overlaps well with developing π-system of the phenol solvolysis product (Figure 6). In contrast, the cyclopropane bond extending to the more-substituted carbon is less effectively aligned and nearly orthogonal to the π-system. Reflecting this relative alignment, the cleaved C8b−C9 bond is the longest (1.544 versus 1.521 Å) and weakest of these two bonds. Thus, the cyclopropane cleavage occurs under stereoelectronic control with preferential addition of the nucleophile at the least-substituted carbon (>20:1). This stereoelectronic control overrides any intrinsic electronic preference for ring expansion ring opening with partial positive charge development on the more substituted cyclopropane carbon but may also benefit from the characteristic preference for S_N2 nucleophilic attack to occur at the least-substituted carbon.

In contrast, the previously obtained X-ray structure[18] for *N*-BOC-CBQ (**9**) containing the six-membered C-ring revealed that the cyclopropane is ideally conjugated and aligned with the π-system and the two potential cyclopropane cleavage bonds are perfectly bisected by the cyclohexadienone π-system (Figure 6). Such a bond orientation is consistent with the loss of solvolytic regioselectivity for *N*-BOC-CBQ which shows only a slight preference for nucleophilic addition at the less-substituted cyclopropane carbon (3:2). Given an inherent preference for partial positive charge delocalization onto a secondary versus primary center, one might have anticipated preferential cleavage of the C9b−C10a bond. However, the bond extending to the less-substituted cyclopropyl carbon is weaker as judged by its longer bond length (1.543 Å versus 1.528 Å) suggesting that any inherent preference for cleavage of the C9b−C10a bond is offset by this lower bond strength of the C9b−C10 bond. In addition, S_N2 nucleophilic attack at the more-substituted tertiary center is sterically disfavored. Given that the ring expansion solvolysis occurs with clean inversion of stereochemistry, the developing torsional strain that accompanies nucleophilic addition with ring expansion may be especially significant and also contributing to the small regioselectivity preference.

(29) Boger, D. L.; McKie, J. A.; Cai, H.; Cacciari, B.; Baraldi, P. G. *J. Org. Chem.* **1996**, *61*, 1710. Boger, D. L.; Han, N.; Tarby, C. M.; Boyce, C. W.; Cai, H.; Jin, Q.; Kitos, P. A. *J. Org. Chem.* **1996**, *61*, 4894.

(30) Boger, D. L.; Jenkins, T. J. *J. Am. Chem. Soc.* **1996**, *118*, 8860.

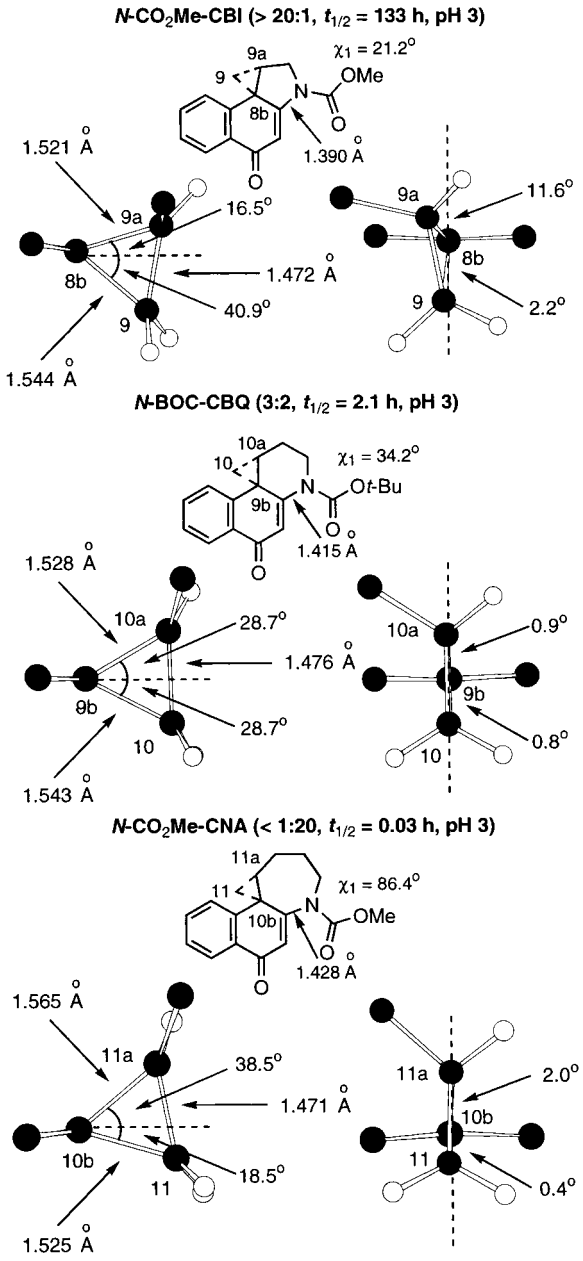

Figure 6. Stick models of the side view and 90° rotation view of the activated cyclopropane of *N*-CO$_2$Me-CBI, *N*-BOC-CBQ, and *N*-CO$_2$Me-CNA illustrating data taken from the X-ray crystal structures and highlighting the stereoelectronic and geometric alignment of the cyclopropane with the cyclohexadienone π-system.

Inspection of the X-ray crystal structure of *N*-CO$_2$Me-CNA reveals that the cyclopropane possesses alignment features of both *N*-CO$_2$Me-CBI and *N*-BOC-CBQ (Figure 6). Like *N*-CO$_2$Me-CBI, the cyclopropane is nonideally conjugated with the π-system but rises above rather than dips below the plane of the cyclohexadienone such that now the bond to the more-substituted cyclopropane carbon enjoys the better stereoelectronic alignment. Thus, the smooth reversal of solvolysis regioselectivity with *N*-BOC-CNA may be attributed to the relative stereoelectronic alignment of the breaking C10b−C11a bond combined with any intrinsic electronic stabilization inherent in its greater substitution. Notably, this combination of stereoelectronic and electronic features is sufficient to overcome the destabilizing steric interactions that must accompany S_N2 addition at the more substituted center. Diagnostic of the regioselectivity of nucleophilic addition, the cleaved C10b−C11a bond is longer (1.565 Å versus 1.525 Å) and weaker than the C10b−C11 bond extending to the less-substituted cyclopropane carbon. Like the geometric alignment of *N*-BOC-CBQ but unlike *N*-BOC-CBI, *N*-CO$_2$Me-CNA possesses a near perfect geometric orientation with respect to the plane bisecting the cyclohexadienone, deviating little from a perfect backside alignment (Figure 6).

Thus, consistent with comparisons that can be made from all such structural studies to date,[11,18,26,29,30] the solvolysis reaction regioselectivity accurately reflects the relative stereoelectronic alignment of the two available cyclopropane bonds. This is beautifully illustrated with the clean, smooth, and complete reversal of the reaction regioselectivity as one progresses through the series *N*-BOC-CBI (>20:1), *N*-BOC-CBQ (3:2), and *N*-BOC-CNA (<1:20).

X-ray Structural Correlations with Solvolysis Reactivity. The solvolysis reactivity increases that occur in the series CNA > CBQ > CBI (Table 1) are the consequence of a previously unappreciated structural feature of the CC-1065 and duocarmycin alkylation subunits. Although the alkylation subunit vinylogous amide has been recognized as a structural feature contributing to its unusual stability, the extent of this stabilization has not been established nor has the structural, chemical, and biological consequences of its presence or disruption been defined.[5] We recently highlighted that one of the most prominent structural features of the alkylation subunits that is directly observable in their X-ray structures is the alternating shortened and lengthened bonds within the vinylogous amide with the most diagnostic feature being the shortened C−N bond length.[31] This provides the opportunity to establish by X-ray the relative extent of the vinylogous amide conjugation that accompanies structural modifications within the alkylation subunit and, ultimately, the ability to correlate this with the properties and chemical reactivity of the agents. Such comparisons within the CBI, CBQ, and CNA series proved especially revealing.

The direct comparisons of the full set of X-ray structures in the series provide a superb assessment of the extent of vinylogous amide conjugation and ultimately, the relative reactivity of the agents. First, *N*-acylation (*e.g.*, *N*-CO$_2$Me-CBI versus CBI) reduces the vinylogous amide conjugation, lengthens bond c, and results in a substantial increase in reactivity. This is observed with each of the three sets of agents (Figure 7). Typical C−N bond lengths for a fully conjugated vinylogous amide are 1.312−1.337 Å.[32] Thus, that of CBI (bond c, 1.337 Å) is diagnostic of a fully engaged vinylogous amide while that of *N*-CO$_2$Me-CBI (1.390 Å) is substantially diminished. Accompanying this reduction in the vinylogous amide conjugation that results from *N*-acylation is an increase in length of the reacting cyclopropane bonds and a readjustment of the cyclopropane alignment to a more idealized conjugation with the cyclohexadienone π-system. This illustrates that both the cyclopropane conjugation and its inherent reactivity increase as the cross-conjugated vinylogous amide π-overlap is diminished. One of the more important conclusions that can be drawn from these correlations is that the pronounced solvolysis

(31) Boger, D. L.; Garbaccio, R. M. *Bioorg. Med. Chem.* **1997**, *5*, 263.
(32) *The Chemistry of Enamines*; Rappaport, Z., Ed.; Wiley: New York, 1994; Part 1.

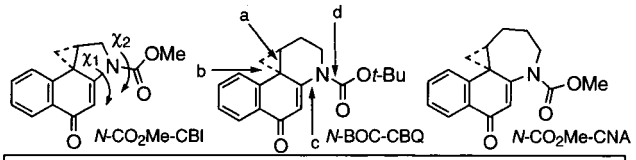

X-ray bond lengths, Å	*N*-CO_2Me-CBI	*N*-BOC-CBQ	*N*-CO_2Me-CNA
a	1.521	1.528	1.565
b	1.544	1.543	1.525
c	1.390	1.415	1.428
d	1.372	1.379	1.357
X-ray dihedral angles			
χ_1	21.2°	34.2°	86.4°
χ_2	4.5°	8.7°	3.9°
solvolysis reactivity			
$t_{1/2}$, (pH 3)	133 h	2.1 h	0.028 h
$t_{1/2}$, (pH 7)	stable	544 h	2.1 h

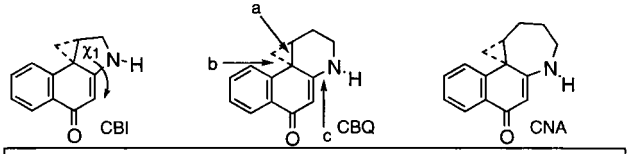

X-ray bond lengths, Å	CBI	CBQ	CNA
a	1.508	1.525	1.543
b	1.532	1.539	1.551
c	1.337	1.336	1.376
X-ray dihedral angle			
χ_1	15.7°	6.9°	50.7°
solvolysis reactivity			
$t_{1/2}$, (pH 3)	930 h	91 h	0.62 h
$t_{1/2}$, (pH 7)	stable	stable	563 h

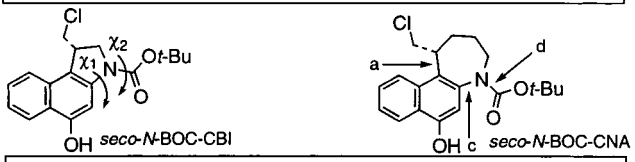

X-ray bond lengths, Å	*seco*-*N*-BOC-CBI	*seco*-*N*-BOC-CNA
a	1.512	1.516
c	1.405	1.422
d	1.353	1.344
X-ray dihedral angle		
χ_1	1.2°	62.8°
χ_2	4.5°	10.1°

Figure 7.

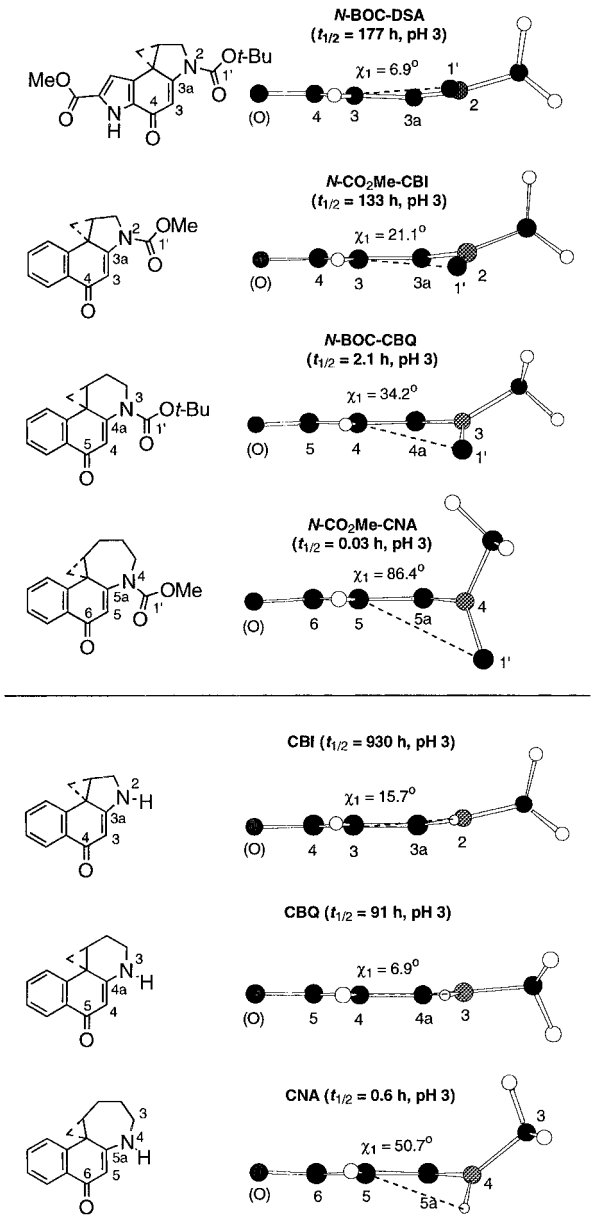

Figure 8. Stick models of the vinylogous amide profile illustrating data taken from X-ray crystal structures and highlighting the χ_1 twist angle of the vinylogous amide. (Note: corresponding dihedral angle incorporating N−H is the same assuming sp^2 hybridization.)

stability of the free NH derivatives is due to this cross-conjugated and fully engaged vinylogous amide. Despite their increased basicity which would facilitate C-4 carbonyl protonation, they are much less reactive than the corresponding *N*-acyl derivatives toward acid-catalyzed nucleophilic addition reactions.[28]

More importantly, these same trends are observed within the *N*-acyl series. As one moves across the series of *N*-CO_2Me-CBI, *N*-BOC-CBQ, and *N*-CO_2Me-CNA, the length of bond c increases (1.390, 1.415, and 1.428 Å) diagnostic of the loss of the cross-conjugated vinylogous amide (Figure 7). Correspondingly, the length, conjugation, and reactivity of the scissile cyclopropane bonds increase tracking with the relative reactivity of the agents. Accompanying these changes and responsible for this loss of vinylogous amide conjugation is an increase in the χ_1 dihedral angle (Figures 7 and 8). Notably, the χ_1 dihedral angle of *N*-CO_2Me-CNA is so large that the acyl group is nearly perpendicular to the plane of the cyclohexadienone π-system, and the agent benefits from little, if any, vinylogous amide conjugation. This is reflected in its bond c length of 1.428 Å. Throughout this series, the χ_2 dihedral angle is maintained at *ca.* 0°, illustrating the preferential maintenance of the N carbamate conjugation versus that of the vinylogous amide. However, *N*-BOC-CBQ exhibits a slightly larger χ_2 dihedral angle, suggesting some carbamate distortion in efforts to maintain the vinylogous amide conjugation. These observations have important implications on the source of catalysis for the DNA alkylation reaction which is discussed in the following section.

An additional and more subtle structural feature that contributes to reactivity is seen in the structural comparisons of the NH derivatives. This series does not

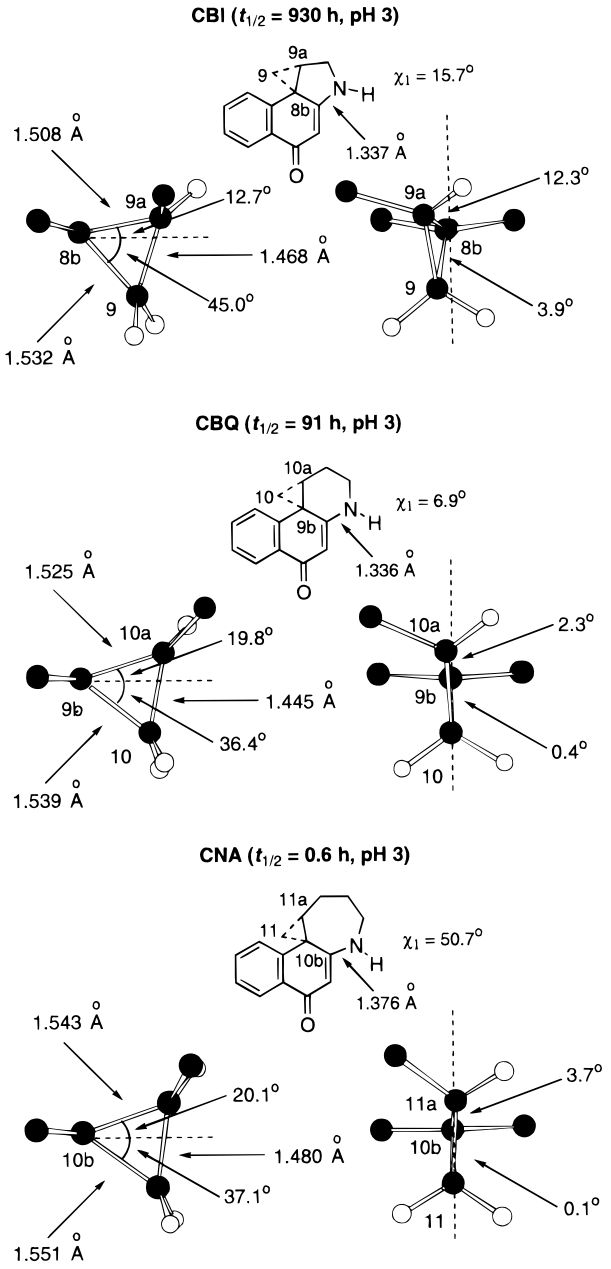

Figure 9. Stick models of the side view and 90° rotation view of the activated cyclopropane of CBI, CBQ, and CNA illustrating data taken from the X-ray crystal structures and highlighting the stereoeloectronic and geometric alignment of the cyclopropane with the cyclohexadienone π-system.

exhibit a completely smooth correlation between the χ_1 torsion angle, the length of bond c, and reactivity (Figure 7). CBI boasts a torsion angle of 15.7° but is significantly less reactive than CBQ which has a smaller torsion angle of 6.9°. In the case of the NH derivatives, the X-ray χ_1 torsional angles reveal nothing about the pyramidalization of the nitrogen and the resulting orientation of its lone pair. Therefore, it is difficult to assess the relative extent of π-overlap simply by measuring the χ_1 angle. However, the identical C−N bond lengths for CBI and CBQ suggest that both benefit from comparable vinylogous amide conjugation. The structural difference that accounts for their 10-fold different reactivities lies in the lengths of the scissile cyclopropyl bonds (Figure 9). CBI has bond lengths of 1.508 Å and 1.532 Å for the C8b−C9a and C8b−C9 bonds, respectively, while those of CBQ are 1.525 Å and 1.539 Å. In turn, this may be attributed to the perfect geometrical (backside) alignment of the CBQ cyclopropane not accessible to CBI.[18] Presumably, this increases the CBQ cyclopropane conjugation, lengthens the scissile cyclopropane bonds, and results in an increased reactivity. In contrast to CBI and CBQ which have similar c bond lengths but different cyclopropyl alignments, CBQ and CNA have similar cyclopropyl alignments but substantially different χ_1 dihedral angles and different c bond lengths of 1.336 versus 1.376 Å, respectively. This difference, diagnostic of the extent of vinylogous amide conjugation, is accompanied by a large increase in the CNA scissile cyclopropane bond lengths indicative of a much greater degree of conjugation and accounts for over a hundred-fold difference in reactivity. Thus, the degree of cyclopropane conjugation and its resulting reactivity is not only related to its geometrical alignment but also to the extent of the cross-conjugated vinylogous amide stabilization.

Thus, the geometrical constraints imposed by the fused five-membered C-ring found in the natural products dictate the regioselectivity of cleavage of the cyclopropane ring. More importantly, the agents display a beautiful interplay between the cross-conjugated stability provided by the vinylogous amide and the extent of cyclopropane conjugation that is central to their functional reactivity. Structural perturbations that diminish the vinylogous amide conjugation increase the cyclopropyl conjugation and its inherent reactivity. One particularly important structural perturbation is the χ_1 dihedral angle of the linking amide of the *N*-acyl derivatives of the alkylation subunits. As the χ_1 dihedral angle is increased, the nitrogen lone pair remains conjugated with the acyl group carbonyl disrupting the vinylogous amide conjugation resulting in very substantial increases in the cyclopropane reactivity. One fundamental insight gained from these comparisons is the extent of the vinylogous amide conjugation and the contribution it makes to the unusual stability of the CBI and DSA alkylation subunits.

Catalysis of the DNA Alkylation Reaction. The remarkable chemical stability of **1**-**3** and the acid-catalysis requirement for addition of typical nucleophiles have led to the assumption that the DNA alkylation must also be an acid-catalyzed reaction. Although efforts have gone into supporting the extent and role of this acid catalysis,[27] it remains largely undocumented for the DNA alkylation reaction. At pH 7.4, the DNA phosphate backbone is fully ionized (0.0001−0.00004% protonated). Consequently, it is unlikely that the catalysis is derived from a phosphate backbone delivery of a proton to the C4 carbonyl as advanced in related efforts.[6] Although increases in the local hydronium ion concentrations surrounding "acidic domains" of DNA have been invoked to explain DNA-mediated acid-catalysis,[33] nucleotide reactivity,[33] and extrapolated in studies with **1** to alkylation site catalysis,[27] the remarkable stability of **1**−**3** even at pH 5 suggests that it is unlikely to be the source of catalysis. Consistent with this, the rate of the DNA alkylation reaction exhibits only a very modest pH dependence below pH 7 and essentially no dependence in the more relevant pH 7−8 range.[11,13]

In conjunction with the results of these studies which document the lack of pH dependence on the rate of DNA

(33) Jayaram, B.; Sharp, K. A.; Honig, B. *Biopolymers* **1989**, *28*, 975. Lamm, G.; Pack, G. R. *Proc. Natl. Acad. Sci. U.S.A.* **1990**, *87*, 9033. Lamm, G.; Wong, L.; Pack, G. R. *J. Am. Chem. Soc.* **1996**, *118*, 3325.

alkylation and related studies that demonstrated that a rigid N^2 amide substituent is required for catalysis,[11,12] an alternative source of catalysis became apparent. The studies detailed herein along with a number of additional unrelated observations have led us to propose that catalysis for the DNA alkylation reaction is derived from a DNA binding-induced conformational change in the agent that disrupts the vinylogous amide stabilization of the alkylation subunit and activates the agent for nucleophilic addition.[31] This conformational change results from adoption of a helical bound conformation that follows the curvature and pitch of the DNA minor groove. The helical rise in the bound conformation of the rigid agents is adjusted by twisting the linking N^2 amide which is the only available flexible site. The twisting of the χ_1 dihedral angle of the linking amide ($\chi_2 \sim 0°$) diminishes the N^2 lone pair conjugation with the cyclohexadienone, disrupts the vinylogous amide stabilization of the alkylation subunit, and increases its inherent reactivity. An alternative possibility involves a twisting of the χ_2 dihedral angle, diminishing the amide conjugation and increasing the N^2 vinylogous amide conjugation. This would increase the basicity of the C4 carbonyl leading to more effective protonation. Notably, both are consistent with the studies that demonstrate even subtle perturbations in the vinylogous amide have a remarkably large impact on reactivity ($\rho = -3.0$).[34] Although our present studies do not directly distinguish between these two possibilities, the latter reflects changes that occur upon *N*-deacylation (*e.g.*, *N*-BOC-CBI to CBI, decreased reactivity) while the former reflects the changes observed in going to the product of the reaction (fully engaged amide, $\chi_2 = 0°$; no vinylogous amide, $\chi_1 \sim 20-35°$ and lengthened bond c). It is consistent with a DNA bound conformation of duocarmycin SA established by ^{1}H NMR which exhibited at 44 ± 2° twist between the planes of the two subunits with the bulk of the twist being accommodated in χ_1.[35] The remarkably large and appropriate reactivity changes observed herein that accompany such a decoupling of the vinylogous amide including that resulting from a twist in the χ_1 dihedral angle is consistent with this as a source of catalysis. The reactivity of *N*-CO_2Me-CNA is extraordinary exhibiting a $t_{1/2}$ of only 2.1 h at pH 7 in the absence of deliberate added acid catalysis. It is $10^3-10^4\times$ more reactive than *N*-BOC-DSA and represents an agent that benefits from little, if any, vinylogous amide stabilization. This level of reactivity is greater than that required. In fact, it is the reactivity and χ_1 dihedral angle of *N*-BOC-CBQ that may more closely approximate that required for the DNA alkylation catalysis provided by the DNA binding-induced conformational change in **1**−**3**. Its inherent reactivity at pH 7 coupled with the rate enhancements afforded a bound species that might provide a further $10^2\times$ rate acceleration approximating the rates observed with the DNA alkylation reaction.

Table 3. In Vitro Cytotoxic Acitivity

agent	configuration	IC_{50} (L1210)
(+)-*N*-BOC-CNA	natural	5 μM (4 μM)[a]
(−)-*N*-BOC-CNA	unnatural	16 μM (29 μM)[a]
(+)-CNA-TMI	unnatural	10 μM (11 μM)[a]
(−)-CNA-TMI	natural	1 μM (0.4 μM)[a]

[a] The value in parentheses is the IC_{50} value for the corresponding *seco*-precusor.

This has important ramifications on the source of the DNA alkylation selectivity. The inherent twist and helical rise of the bound conformation of the agent is greatest within the narrower, deeper AT-rich minor groove. This leads to preferential activation of the agent for DNA alkylation within extended AT-rich minor groove sites and complements their preferential AT-rich noncovalent binding selectivity.[36] Thus, both shape-selective recognition (preferential AT-rich noncovalent binding) and shape-dependent catalysis (extended AT-rich > GC-rich activation by twist in N^2 amide) combine to restrict S_N2 alkylation to accessible adenine N3 nucleophilic sites within the preferred binding sites. Importantly, this ground state destabilization of the substrate only activates the agent for a rate determining S_N2 nucleophilic addition and requires the subsequent proper positioning and accessibility to an adenine N3 site.

This source of catalysis requires an extended and rigid N^2 amide substituent,[12] and the absence of such a substituent with **4**−**6** accounts nicely for their slow and ineffective DNA alkylation. The noncovalent binding derived from the attached right-hand subunits accounts for a much smaller part of the difference in the rates of DNA alkylation between **4**−**6** and **1**−**3**.[12] More importantly, this source of catalysis would lead to distinctions, not similarities, in the DNA alkylation selectivities of **4**-**6** versus **1** contrary to the consequences of alternative proposals that have been advanced.[6,10,37]

In Vitro Cytotoxic Activity. The in vitro cytotoxic activity of the agents proved to be consistent with past observations that have illustrated a direct correlation between solvolysis stability and cytotoxic potency. The CNA-based agents exhibited cytotoxic activity that was less potent than the corresponding duocarmycin-based agents but more potent than the corresponding CI-based agents (Table 3 and Figure 10). The natural enantiomers of the CNA-based agents were found to be more potent than the unnatural enantiomers.[38] Interestingly, the natural enantiomer of the full analog of duocarmycin SA, CNA-TMI (**30**), was only $5-10\times$ more potent than *N*-BOC-CNA (**10**), and the difference in potency of the unnatural enantiomers was even smaller ($1-2\times$). While this may simply be due to the extraordinary reactivity of the agents which preclude effective DNA alkylation,

(34) Boger, D. L.; Yun, W. *J. Am. Chem. Soc.* **1994**, *116*, 5523. The increased stability and decreased acid-catalyzed solvolysis reactivity that smoothly correlates with the electron-withdrawing strength of the N^2 substituent detailed in this work suggests the interesting possibility that solvolysis catalysis may be derived from protonation of the N^2 acyl substituent carbonyl rather than C4 carbonyl protonation. The net effect of this protonation would be further deconjugation of the vinylogous amide. Moreover, the rate of solvolysis would be dependent upon the relative ease of protonation of the N^2 acyl substituent carbonyl ($CONH_2 > CO_2CH_3 > COCH_3$).

(35) Eis, P.; Smith, J. A.; Rydzewski, J. M.; Case, D. A.; Boger, D. L.; Chazin, W. J. *J. Mol. Biol.*, in press.

(36) Boger, D. L.; Coleman, R. S.; Invergo, B. J.; Zarrinmayeh, H.; Kitos, P. A.; Thompson, S. C.; Leong, T.; McLaughlin, L. W. *Chem. Biol. Interact.* **1990**, *73*, 29. Boger, D. L.; Zhou, J.; Cai, H. *Bioorg. Med. Chem.* **1996**, *4*, 859.

(37) Lin, C. H.; Sun, D.; Hurley, L. H. *Chem. Res. Toxicol.* **1991**, *4*, 21. Lee, C.-S.; Sun, D.; Kizu, R.; Hurley, L. H. *Chem. Res. Toxicol.* **1991**, *4*, 203. Lin, C. H.; Hill, G. C.; Hurley, L. H. *Chem. Res. Toxicol.* **1992**, *5*, 167. Ding, Z.-M.; Harshey, R. M.; Hurley, L. H. *Nucl. Acids Res.* **1993**, *21*, 4281. Sun, D.; Lin, C. H.; Hurley, L. H. *Biochemistry* **1993**, *32*, 4487. Thompson, A. S.; Sun, D.; Hurley, L. H. *J. Am. Chem. Soc.* **1995**, *117*, 2371.

(38) The tentative assignment of the absolute configuration of CNA-TMI (**30**) is based on both the more potent cytotoxic activity and the DNA alkylation selectivity of (−)-CNA-TMI which corresponds to that of the natural enantiomers. The potential that this may be reversed by virtue of the reversed regioselectivity of adenine N3 nucleophilic addition is presently under investigation.

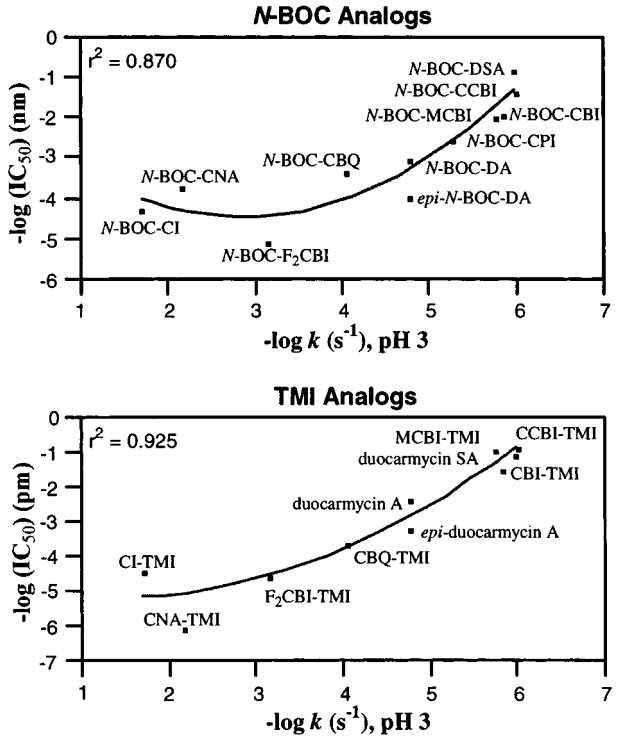

Figure 10.

this also suggests that the twisted conformation of the full analogs may be sufficient to disfavor minor groove binding providing agents that are comparable to analogs lacking the attached DNA binding subunits altogether.

Experimental Section

4-(Benzyloxy)-*N*-(*tert*-butyloxycarbonyl)-1-iodo-*N*-(4-penten-1-yl)-2-naphthylamine (13). A solution of **12**[19] (1.00 g, 2.11 mmol, 1 equiv) in benzene (100 mL) was treated with 50% w/v aqueous NaOH (20 mL). Benzyltributylammonium chloride (1.32 g, 4.22 mmol, 2 equiv) was added followed by 5-[(methanesulfonyl)oxy]-1-pentene (1.73 g, 10.53 mmol, 5 equiv). The resulting biphasic mixture was stirred vigorously at 25 °C for 12 h. The layers were allowed to separate, and the aqueous portion was extracted with EtOAc (2 × 30 mL). The combined organic portions were washed with H_2O (2 × 100 mL) and saturated aqueous NaCl (50 mL). Drying ($MgSO_4$), filtration, and concentration was followed by flash chromatography (SiO_2, 3.5 × 14 cm, 5% EtOAc−hexane) to furnish **13** (0.975 g, 1.15 g theoretical, 85%) as a pale yellow solid: mp 69−71 °C; ^{1}H NMR (500 MHz, $CDCl_3$) major rotamer δ 8.34−8.32 (m, 1H), 8.23−8.21 (m, 1H), 7.62−7.49 (m, 4H), 7.42−733 (m, 3H), 6.70 (s, 1H), 5.81−5.71 (m, 1H), 5.34−5.18 (m, 2H), 5.01−4.93 (m, 2H), 3.84 (ddd, J = 17.5, 12.6, 7.6 Hz, 1H), 3.37−3.31 (m, 1H), 2.07−2.02 (m, 2H), 1.74−1.65 (m, 2H), 1.31 (s, 9H); ^{13}C NMR (125 MHz, $CDCl_3$) major rotamer δ 155.1, 154.0, 143.2, 137.9, 136.4, 135.4, 132.8, 128.7 (2C), 128.5, 128.2 (2C), 127.2, 126.2, 122.5, 115.0, 107.8, 95.1, 80.1, 70.3, 49.1, 31.3, 28.6, 28.3 (3C), 27.5; IR (film) ν_{max} 3067, 3036, 2974, 2923, 1697, 1615, 1590 cm^{-1}; FABHRMS (NBA−NaI) m/z 544.1337 (M + Na^+, $C_{27}H_{30}INO_3$ requires 544.1349). Anal. Calcd for $C_{27}H_{30}INO_3$: C, 59.65; H, 5.57; N, 2.58. Found C, 60.02; H, 5.27; N, 2.54.

7-(Benzyloxy)-5-(*tert*-butyloxycarbonyl)-1-methylidene-1,2,3,4-tetrahydro-5*H*-naphtho[1,2−*b*]azepine (14). A solution of **13** (0.503 g, 0.926 mmol, 1 equiv) in CH_3CN (18 mL, 0.051 M, degassed and purged with Ar) in a thick-walled reaction tube was treated with Et_3N (0.257 mL, 1.85 mmol, 2 equiv) followed by $(Ph_3P)_4Pd$ (0.032 g, 0.0277 mmol, 0.03 equiv). The reaction vessel was sealed, and the mixture was warmed at 130 °C for 14 h. Concentration gave a yellow semisolid that was suspended in 5% EtOAc−hexanes. The precipitated salts were removed by filtration and thoroughly rinsed with the solvent mixture. Concentration of the filtrate and radial chromatography (SiO_2, 2 mm plate, 5% EtOAc-hexane) afforded **14** as a colorless oil (0.343 g, 0.384 g theoretical, 89%) which slowly crystallized upon storage: mp 99−100 °C; ^{1}H NMR (400 MHz, $CDCl_3$) major rotamer δ 8.37−8.35 (m, 1H), 8.13−8.11 (m, 1H), 7.54−7.34 (m, 7H), 6.72 (s, 1H), 5.52 (s, 1H), 5.24 (s, 2H), 4.94 (s, 1H), 4.50−4.10 (m, 1H), 3.70−3.30 (m, 1H), 2.95−1.70 (m, 4H), 1.26 (s, 9H); ^{13}C NMR (100 MHz, $CDCl_3$) major rotamer δ 153.1, 145.3, 137.2, 137.0, 132.2, 129.8, 128.7 (3C), 128.0 (2C), 127.7, 127.2, 126.6, 126.1, 124.9, 122.1, 117.3, 106.5, 79.7, 70.2, 47.4, 35.1, 29.8, 28.3 (3C); IR (film) ν_{max} 3071, 3031, 2971, 2931, 2852, 1694, 1590 cm^{-1}; FABHRMS (NBA−NaI) m/z 438.2065 (M + Na^+, $C_{27}H_{29}NO_3$ requires 438.2045).

7-(Benzyloxy)-5-(*tert*-butyloxycarbonyl)-1-(hydroxymethyl)-1,2,3,4-tetrahydro-5*H*-naphtho[1,2−*b*]azepine (15). A solution of **14** (0.209 g, 0.504 mmol, 1 equiv) in THF (5 mL) was cooled to 0 °C prior to dropwise addition of BH_3•SMe_2 (0.151 mL, 10 M, 3(9) equiv). The cooling bath was removed after 5 min, and the mixture was stirred at 25 °C for 12 h. The excess borane was quenched with slow addition of H_2O (0.6 mL). Oxidative workup was accomplished by the addition of 2.5 M aqueous NaOH (0.605 mL, 3 equiv) followed by 30% H_2O_2 (0.514 mL, 9 equiv), and the resulting heterogeneous solution was stirred rapidly at 25 °C (1 h) and 50 °C (1 h). The cooled reaction mixture was treated with saturated aqueous NaCl (0.5 mL), and the layers were separated. The aqueous portion was extracted with EtOAc (2 × 5 mL), and the combined organic portions were dried ($MgSO_4$), filtered, and concentrated. Radial chromatography (SiO_2, 2 mm plate, 30% EtOAc−hexane) provided **15** as a colorless oil (0.179 g, 0.218 g theoretical, 82%) which slowly crystallized upon storage: mp 108−110 °C; ^{1}H NMR (400 MHz, $CDCl_3$) major rotamer δ 8.40 (d, J = 8.3 Hz, 1H), 8.18 (d, J = 8.6 Hz, 1H), 7.57−7.34 (m, 7H), 6.62 (s, 1H), 5.28 (d, J = 12.1 Hz, 1H), 5.17 (d, J = 12.0 Hz, 1H), 4.41−4.37 (m, 1H), 4.09−4.06 (m, 1H), 3.88−3.86 (m, 2H), 2.81−2.75 (m, 1H), 2.23−2.03 (m, 2H), 1.71−1.48 (m, 3H), 1.29 (s, 9H); ^{13}C NMR (100 MHz, $CDCl_3$) major rotamer δ 154.0, 153.2, 139.9, 136.9, 133.6, 128.7 (2C), 128.0 (2C), 127.7, 127.0 (2C), 125.4, 125.0, 123.7, 122.7, 107.3, 80.2, 70.1, 63.3, 47.5, 39.1, 28.3 (3C), 26.3, 24.1; IR (film) ν_{max} 3429, 3067, 3037, 2967, 2926, 2866, 1694, 1674, 1619, 1594 cm^{-1}; FABHRMS (NBA−CsI) m/z 566.1333 (M + Cs^+, $C_{27}H_{31}NO_4$ requires 566.1307). Anal. Calcd for $C_{27}H_{31}NO_4$: C, 74.79; H, 7.21; N, 3.23. Found: C, 74.49; H, 7.37; N, 3.44.

7-(Benzyloxy)-5-(*tert*-butyloxycarbonyl)-1-[((methanesulfonyl)oxy)methyl]-1,2,3,4−tetrahydro-5*H*-naphtho[1,2−*b*]azepine (16). A solution of **15** (0.138 g, 0.319 mmol, 1 equiv) in CH_2Cl_2 (3 mL) was cooled to 0 °C prior to sequential addition of Et_3N (0.222 mL, 1.59 mmol, 5 equiv) and CH_3SO_2Cl (0.049 mL, 0.637 mmol, 2 equiv). The cooling bath was removed after 5 min, and the mixture was stirred at 25 °C for 1 h. The reaction was quenched with the addition of saturated aqueous $NaHCO_3$ (0.5 mL), and the layers were separated. The aqueous portion was extracted with EtOAc (2 × 5 mL), and the combined organic portions were dried ($MgSO_4$), filtered, and concentrated. Radial chromatography (SiO_2, 2 mm plate, 30% EtOAc−hexane) furnished **16** (0.143 g, 0.163 g theoretical, 89%) as a white solid: mp 134−135 °C; ^{1}H NMR (400 MHz, $CDCl_3$) major rotamer δ 8.40 (d, J = 8.2 Hz, 1H), 8.13 (d, J = 8.6 Hz, 1H), 7.60−7.35 (m, 7H), 6.63 (s, 1H), 5.26 (d, J = 11.7 Hz, 1H), 5.17 (d, J = 11.6 Hz, 1H), 4.49−4.44 (m, 2H), 4.38−4.30 (m, 2H), 2.69−2.64 (m, 4H), 2.26−2.05 (m, 2H), 1.73−1.70 (m, 2H), 1.32 (s, 9H); ^{13}C NMR (100 MHz, $CDCl_3$) major rotamer δ 153.8, 153.6, 140.5, 136.7, 133.0, 128.8 (2C), 128.6, 128.1 (2C), 127.7, 127.6, 127.1, 125.2, 123.3, 122.8, 107.1, 80.8, 71.4, 70.2, 47.7, 37.1, 36.1, 28.3 (3C), 26.5, 24.4; IR (film) ν_{max} 3056, 2974, 2933, 2862, 1692, 1615, 1590 cm^{-1}; FABHRMS (NBA−NaI) m/z 534.1914 (M + Na^+, $C_{28}H_{33}NO_6S$ requires 534.1926). Anal. Calcd for $C_{28}H_{33}NO_6S$: C, 65.73; H, 6.51; N, 2.74; S, 6.25. Found: C, 65.68; H, 6.59; N, 2.55; S, 6.31.

A solution of **16** (0.055 g) in 50% *i*-PrOH−hexane was resolved on a semipreparative Diacel Chiracel OD column (10 μm, 2 × 25 cm) using 10% *i*-PrOH−hexane as eluent (7 mL/min). The effluent was monitored at 254 nm and the enan-

tiomers eluted with retention times of 38.0 and 45.0 min, respectively (α = 1.18). The fractions were collected and concentrated to afford *ent*-(+)-(1*S*)-**16** (t_R = 38.0 min, 0.0251 g) and (−)-(1*R*)-**16** (t_R = 45.0 min, 0.0248 g) with a 91% recovery (>99.9% ee).

(−)-(1*R*)-**16**: $[\alpha]^{25}_D$ −41 (*c* 0.12, $CHCl_3$).

ent-(+)-(1*S*)-**16**: $[\alpha]^{25}_D$ +46 (*c* 0.13, $CHCl_3$).

5-(*tert*-Butyloxycarbonyl)-7-hydroxy-1-[((methanesulfonyl)oxy)methyl]-1,2,3,4−tetrahydro-5*H*-naphtho[1,2−*b*]azepine (17). A solution of **16** (0.096 g, 0.188 mmol, 1 equiv) in THF (3.0 mL) was treated with 10% Pd−C (0.042 g, 0.04 mmol, 0.2 equiv) followed by aqueous HCO_2NH_4 (1.0 mL, 25% w/v, 21 equiv) and the resulting mixture was stirred at 25 °C for 2.5 h. The mixture was filtered through Celite to afford a biphasic filtrate which was partitioned. The aqueous phase was extracted with EtOAc (2 × 2 mL), and the combined organic portions were dried ($MgSO_4$), filtered, and concentrated to give **17** as an analytically pure white solid (0.072 g, 0.079 g theoretical, 91%): mp 141−142 °C; ^{1}H NMR (400 MHz, DMF-d_7) major rotamer δ 8.29 (d, J = 8.2 Hz, 1H), 8.26 (d, J = 8.7 Hz, 1H), 7.62−7.59 (m, 1H), 7.54−7.50 (m, 1H), 6.82 (s, 1H), 4.59−4.47 (m, 1H), 4.43−4.25 (m, 3H), 3.02 (s, 3H), 2.98−2.76 (m, 1H), 2.35−2.20 (m, 1H), 2.13−1.95 (m, 1H), 1.71−1.67 (m, 2H), 1.39 (s, 9H); ^{13}C NMR (100 MHz, DMF-d_7) major rotamer δ 154.0, 153.5, 141.8, 134.0, 127.7, 125.2, 125.1, 124.3, 123.3, 123.0, 110.3, 80.4, 71.4, 48.2, 36.8, 36.4, 28.2 (3C), 27.2, 25.0; IR (film) ν_{max} 3262, 2974, 2933, 2872, 1692, 1662, 1594 cm^{-1}; FABHRMS (NBA−NaI) *m*/*z* 444.1468 (M + Na$^+$, $C_{21}H_{27}NO_6S$ requires 444.1457).

(−)-(1*R*)-**17**: $[\alpha]^{25}_D$ −63 (*c* 0.084, THF).

ent-(+)-(1*S*)-**17**: $[\alpha]^{25}_D$ +58 (*c* 0.084, THF).

7-(Benzyloxy)-5-(*tert*-butyloxycarbonyl)-1-(chloromethyl)-1,2,3,4-tetrahydro-5*H*-naphtho[1,2−*b*]azepine (18). A solution of **15** (0.105 g, 0.24 mmol, 1 equiv) in CH_2Cl_2 (2 mL) was treated with CCl_4 (0.225 mL, 2.33 mmol, 9.7 equiv) followed by Ph_3P (0.212 g, 0.81 mmol, 3.3 equiv), and the mixture was stirred at 25 °C for 2.5 h. The crude reaction solution was passed through a plug of silica gel and concentrated. Radial chromatography (SiO_2, 1 mm plate, 5% EtOAc−hexane) provided **18** as a pale yellow oil (0.048 g, 0.108 g theoretical, 44%): ^{1}H NMR (250 MHz, $CDCl_3$) major rotamer δ 8.44−8.36 (m, 1H), 8.15−7.12 (m, 1H), 7.62−7.33 (m, 7H), 6.64 (s, 1H), 5.31−5.15 (m, 2H), 4.46−4.41 (m, 1H), 4.17−4.08 (m, 1H), 3.92−3.81 (m, 1H), 3.74−3.63 (m, 1H), 2.78−2.69 (m, 1H), 2.41−2.35 (m, 1H), 2.17−2.05 (m, 1H), 1.72−1.67 (m, 2H), 1.30 (s, 9H); IR (film) ν_{max} 2971, 2930, 2859, 1693, 1617, 1592 cm^{-1}; FABHRMS (NBA−NaI) *m*/*z* 451.1933 (M$^+$, $C_{27}H_{30}ClNO_3$ requires 451.1914).

5-(*tert*-Butyloxycarbonyl)-1-(chloromethyl)-7-hydroxy-1,2,3,4-tetrahydro-5*H*-naphtho[1,2−*b*]azepine (19). A solution of **18** (0.043 g, 0.095 mmol, 1 equiv) in THF (1.5 mL) was treated with 10% Pd−C (0.020 g, 0.019 mmol, 0.2 equiv) followed by aqueous HCO_2NH_4 (0.5 mL, 25% w/v, 1.98 mmol, 21 equiv), and the resulting black suspension was stirred rapidly at 25 °C for 2.5 h. The crude mixture was filtered through a plug of Celite to afford a biphasic filtrate which was partitioned. The aqueous portion was extracted with EtOAc (2 × 1 mL), and the combined organic portions were dried ($MgSO_4$), filtered, and concentrated to provide **19** as an analytically pure white solid (0.032 g, 0.034 g theoretical, 94%). Recrystallization from 10% EtOAc−hexane gave colorless plates suitable for X-ray analysis:[24] mp 157−159 °C; ^{1}H NMR (400 MHz, $CDCl_3$) major rotamer δ 7.98−7.94 (m, 1H), 7.37−7.32 (m, 1H), 7.22−7.19 (m, 1H), 6.96−6.90 (m, 1H), 6.47 (s, 1H), 4.41−4.26 (m, 1H), 4.19−4.07 (m, 1H), 3.89−3.81 (m, 2H), 2.88−2.78 (m, 1H), 2.51−2.46 (m, 1H), 2.18−2.05 (m, 1H), 1.71−1.67 (m, 2H), 1.40 (s, 9H); ^{1}H NMR (400 MHz, acetone-d_6) major rotamer δ 9.17 (s, 1H), 8.27 (d, J = 8.1 Hz, 1H), 8.19−8.17 (m, 1H), 7.59−7.54 (m, 1H), 7.50−7.46 (m, 1H), 6.75 (s, 1H), 4.39−4.36 (m, 1H), 4.19−4.15 (m, 1H), 3.92−3.87 (m, 1H), 3.75−3.63 (m, 1H), 2.75−2.68 (m, 1H), 2.37−2.33 (m, 1H), 2.06−2.04 (m, 1H), 1.69−1.67 (m, 2H), 1.40 (s, 9H); ^{13}C NMR (100 MHz, $CDCl_3$) major rotamer δ 155.8, 152.9, 151.6, 139.3, 132.3, 126.5, 124.9, 124.7, 123.5, 122.4, 109.4, 81.5, 48.9, 44.6, 38.6, 28.4 (3C), 26.3, 24.2; IR (film) ν_{max} 3287, 2965, 2915, 2844, 1693, 1663 cm^{-1}; FABHRMS (NBA−NaI) *m*/*z* 384.1352 (M + Na$^+$, $C_{20}H_{24}ClNO_3$ requires 384.1342).

A solution of **19** (0.0096 g) in 50% *i*-PrOH−hexane was resolved on a semipreparative Diacel Chiracel OD column (10 μm, 2 × 25 cm) using 6% *i*-PrOH−hexane as eluent (6 mL/min). The effluent was monitored at 254 nm, and the enantiomers were eluted with retention times of 22.6 and 26.8 min, respectively (α = 1.19). The fractions were collected and concentrated to afford (−)-(1*R*)-**19** (t_R = 22.6 min, 0.0033 g) and *ent*-(+)-(1*S*)-**19** (t_R = 26.8 min, 0.0031 g) with a 67% recovery (>99.9% ee). The absolute configuration of (−)-(1*R*)-**19** was established by X-ray analysis.[24]

(−)-(1*R*)-**19**: $[\alpha]^{25}_D$ −67 (*c* 0.017, THF).

ent-(+)-(1*S*)-**19**: $[\alpha]^{25}_D$ +67 (*c* 0.016, THF).

***N*-(*tert*-Butyloxycarbonyl)-1,2,3,4,11,11a-hexahydrocyclopropa[*c*]naphtho[2,1−*b*]azepin-6-one (*N*-BOC-CNA, 10).** A sample of **17** (0.025 g, 0.059 mmol, 1 equiv) was suspended in CH_3CN (1.0 mL) and treated with DBU (0.027 mL, 0.178 mmol, 3 equiv) at 25 °C to instantly afford a homogeneous pale yellow solution. The solvent was removed with a gentle stream of N_2 after 5 min. Flash chromatography (SiO_2, 1 × 7 cm, 30% EtOAc−hexane with 5% Et_3N) furnished **10** as a colorless oil (0.017 g, 0.019 g theoretical, 87%): ^{1}H NMR (400 MHz, CD_3CN) δ 8.12 (dd, J = 7.9, 1.5 Hz, 1H), 7.61 (ddd, J = 8.3, 7.1, 1.5 Hz, 1H), 7.41 (ddd, J = 8.0, 7.2, 1.0 Hz, 1H), 7.14 (d, J = 8.1 Hz, 1H), 6.48 (s, 1H), 4.09−4.02 (m, 1H), 2.69−2.54 (m, 1H), 2.28−2.22 (m, 1H), 2.10−2.07 (m, 2H), 1.95−1.91 (m, 2H overlapping with solvent), 1.75−1.72 (m, 1H), 1.62−1.57 (m, 1H), 1.26 (broad s, 9H); ^{13}C NMR (100 MHz, CD_3CN) δ 186.4, 162.1, 146.8, 133.7, 132.8, 129.3, 126.8, 126.6, 123.3, 81.0, 47.8, 40.2, 33.8, 28.4, 28.3, 26.8 (3C), 26.0, 25.9; IR (film) ν_{max} 2923, 2852, 1698, 1647, 1596 cm^{-1}; UV (THF) λ_{max} 304 (ϵ 8600), 258 (ϵ 11100), 220 (ϵ 15500) nm; FABHRMS (NBA−NaI) *m*/*z* 326.1766 (M + H$^+$, $C_{20}H_{24}NO_3$ requires 326.1756).

(+)-**10**: $[\alpha]^{25}_D$ +36 (*c* 0.009, EtOAc).

ent-(−)-**10**: $[\alpha]^{25}_D$ −36 (*c* 0.016, EtOAc).

1,2,3,4,11,11a-Hexahydrocyclopropa[*c*]naphtho[2,1−*b*]azepin-6-one (CNA, 11). A sample of **17** (0.030 g, 0.07 mmol, 1 equiv) was suspended in 3.9 M HCl−EtOAc (1.5 mL). After 40 min, the volatiles were removed with a gentle stream of N_2 followed by high vacuum. The resulting white foam was dissolved in CH_3CN containing DBU (0.105 mL, 0.70 mmol, 10 equiv in 1 mL of CH_3CN). The solvent was removed with a gentle stream of N_2 after 5 min. Radial chromatography (SiO_2, 1 mm plate, 95% CH_2Cl_2−CH_3OH) furnished **11** as a pale yellow solid (0.012 g, 0.016 g theoretical, 77%). Recrystallization from 10% CH_3OH−CH_3CN gave pale yellow plates suitable for X-ray analysis:[24] mp 180−183 °C with decomposition; ^{1}H NMR (400 MHz, CD_3OD) δ 8.07 (dd, J = 7.8, 1.5 Hz, 1H), 7.50 (ddd, J = 8.7, 7.2, 1.6 Hz, 1H), 7.33 (ddd, J = 8.0, 7.2, 1.0 Hz, 1H), 7.13 (d, J = 8.1 Hz, 1H), 6.00 (s, 1H), 3.54−3.48 (m, 1H), 3.00−2.90 (m, 1H), 2.78−2.74 (m, 1H), 2.50 (dd, J = 8.7, 5.0 Hz, 1H), 2.41−2.36 (m, 1H), 2.24−2.15 (m, 1H), 1.92−1.79 (m, 3H); ^{13}C NMR (150 MHz, CD_3OD) δ 184.6, 175.0, 146.3, 133.0, 132.7, 126.6, 126.1, 122.4, 107.9, 45.4, 38.2, 31.0 (2C), 26.4, 26.1; IR (film) ν_{max} 3285, 2924, 2855, 1608, 1584 cm^{-1}; UV (CH_3OH) λ_{max} 342 (ϵ 11900), 308 (ϵ 8300), 245 (ϵ 17100) nm; FABHRMS (NBA−NaI) *m*/*z* 226.1238 (M + H$^+$, $C_{15}H_{16}NO$ requires 226.1232).

7-(Benzyloxy)-1-methylidene-1,2,3,4-tetrahydro-5*H*-naphthol[1,2−*b*]azepine Hydrochloride (20). A solution of **14** (0.226 g, 0.55 mmol, 1 equiv) was dissolved in 3.9 M HCl−EtOAc (7.0 mL). After 40 min, the volatiles were removed with a gentle stream of N_2 followed by high vacuum. The resulting crude pale green solid was used directly for the synthesis of **21** and **22** without further characterization.

7-(Benzyloxy)-5-(methoxycarbonyl)-1-methylidene-1,2,3,4-tetrahydro-5*H*-naphtho[1,2−*b*]azepine (21). A solution of **20** (0.049 g, 0.14 mmol, 1 equiv) in THF (1.5 mL) was treated with $NaHCO_3$ (0.026 g, 0.31 mmol, 2.2 equiv) followed by methyl chloroformate (0.022 mL, 0.28 mmol, 2.0 equiv), and the mixture was stirred at 25 °C for 5 h. The reaction was quenched with the addition of saturated aqueous $NaHCO_3$ (0.5 mL), and the resulting layers were separated. The aqueous portion was extracted with EtOAc (2 × 2 mL), and the combined organic portions were dried ($MgSO_4$),

filtered, and concentrated. Trituration with 10% EtOAc−hexane furnished **21** as a white solid (0.049 g, 0.052 g theoretical, 94%): mp 99−100 °C; ^{1}H NMR (500 MHz, $CDCl_3$) major rotamer δ 8.38−8.36 (m, 1H), 8.14−8.13 (m, 1H), 7.54−7.36 (m, 7H), 6.73 (s, 1H), 5.56 (s, 1H), 5.25 (s, 2H), 4.99 (s, 1H), 4.50−4.20 (m, 1H), 3.59 (s, 3H), 3.10−2.35 (m, 1H), 2.22−1.70 (m, 4H); ^{13}C NMR (125 MHz, $CDCl_3$) major rotamer δ 155.5, 153.4, 144.7, 136.8, 136.2, 132.2, 129.9, 128.6 (2C), 127.9, 127.3 (2C), 126.8, 126.1, 125.2 (2C), 122.2, 118.0, 105.8, 70.2, 52.8, 48.1, 35.0, 29.7; IR (film) ν_{max} 3067, 2923, 2862, 1703, 1590, 1508 cm^{-1}; FABHRMS (NBA−NaI) *m/z* 373.1688 (M^+, $C_{24}H_{23}NO_3$ requires 373.1678).

7-(Benzyloxy)-1-(hydroxymethyl)-5-(methoxycarbonyl)-1,2,3,4-tetrahydro-5*H*-naphtho[1,2−*b*]azepine (23). Following the general procedure detailed for **15**, **21** (0.049 g, 0.013 mmol, 1 equiv) was treated with BH_3•SMe_2 (0.039 mL, 10 M, 3(9) equiv), quenched with H_2O (0.16 mL), and oxidized with aqueous 2.5 M NaOH (0.16 mL, 0.39 mmol, 3 equiv) and 30% aqueous H_2O_2 (0.134 mL, 9 equiv). Radial chromatography (SiO_2, 1 mm plate, 50% EtOAc−hexane) provided **23** as a white solid (0.033 g, 0.051 g theoretical, 64%): mp 90−92 °C; ^{1}H NMR (500 MHz, $CDCl_3$) major rotamer δ 8.41 (d, J = 8.5 Hz, 1H), 8.18 (d, J = 8.5 Hz, 1H), 7.57−7.35 (m, 7H), 6.63 (s, 1H), 5.25−5.17 (m, 2H), 4.46−4.43 (m, 1H), 4.09−4.07 (m, 1H), 3.87−3.76 (m, 2H), 3.59 (s, 3H), 2.93−2.83 (m, 1H), 2.21−2.08 (m, 2H), 1.70−1.64 (m, 3H); ^{13}C NMR (125 MHz, $CDCl_3$) major rotamer δ 155.6, 153.4, 139.0, 136.7, 133.5, 128.6 (2C), 128.0 (2C), 127.6, 127.3 (3C), 125.2, 123.7, 122.8, 106.9, 70.1, 63.4, 52.9, 48.3, 39.1, 26.4, 24.1; IR (film) ν_{max} 3453, 3063, 3032, 2940, 2868, 1696, 1593 cm^{-1}; FABHRMS (NBA−NaI) *m/z* 392.1871 (M + H^+, $C_{24}H_{25}NO_4$ requires 392.1862).

7-(Benzyloxy)-1-[((methanesulfonyl)oxy)methyl]-5-(methoxycarbonyl)-1,2,3,4−tetrahydro-5*H*-naphtho[1,2−*b*]azepine (25). Following the general procedure detailed for **16**, **23** (0.029 g, 0.074 mmol, 1 equiv) was treated with Et_3N (0.052 mL, 0.371 mmol, 5 equiv) and CH_3SO_2Cl (0.017 mL, 0.148 mmol, 2 equiv). Radial chromatography (SiO_2, 1 mm plate, 50% EtOAc−hexane) furnished **25** (0.032 g, 0.035 g theoretical, 91%) as a white solid: mp 130−132 °C; ^{1}H NMR (500 MHz, $CDCl_3$) major rotamer δ 8.40 (d, J = 8.5 Hz, 1H), 8.13 (d, J = 8.5 Hz, 1H), 7.61−7.35 (m, 7H), 6.63 (s, 1H), 5.27−5.17 (m, 2H), 4.51−4.33 (m, 4H), 3.60 (s, 3H), 2.86−2.81 (m, 1H), 2.54 (s, 3H), 2.32−2.23 (m, 1H), 2.07−2.04 (m, 1H), 1.76−1.70 (m, 2H); ^{13}C NMR (125 MHz, $CDCl_3$) major rotamer δ 155.3, 153.7, 139.5, 136.6, 133.1, 128.6 (2C), 128.0 (2C), 127.7, 127.6, 127.3, 125.4, 124.3, 123.4, 122.8, 106.9, 71.1, 70.1, 53.0, 48.3, 36.8, 36.2, 26.7, 24.5 ; IR (film) ν_{max} 3063, 3022, 2938, 2858, 1701, 1593 cm^{-1}; FABHRMS (NBA) *m/z* 470.1648 (M + H^+, $C_{25}H_{27}NO_6S$ requires 470.1637).

7-Hydroxy-1-[((methanesulfonyl)oxy)methyl]-5-(methoxycarbonyl)-1,2,3,4-tetrahydro-5*H*-naphtho[1,2−*b*]-azepine (27). Following the general procedure detailed for **17**, **25** (0.028 g, 0.060 mmol, 1 equiv) was treated with 10% Pd-C (0.010 g, 0.009 mmol, 0.16 equiv) followed by aqueous HCO_2NH_4 (0.265 mL, 25% w/v, 18 equiv). Filtration and concentration gave **27** as an analytically pure white solid (0.0204 g, 0.0225 g theoretical, 91%): mp 113−115 °C; ^{1}H NMR (500 MHz, CD_3OD) major rotamer δ 8.25 (d, J = 7.5 Hz, 1H), 8.14 (d, J = 8.5 Hz, 1H), 7.55−7.45 (m, 2H), 6.60 (s, 1H), 4.41−4.33 (m, 4H), 3.66 (s, 3H), 2.85−2.79 (m, 1H), 2.64 (s, 3H), 2.35−2.20 (m, 1H), 2.13−1.95 (m, 1H), 1.71−1.67 (m, 2H); ^{13}C NMR (125 MHz, CD_3OD) major rotamer δ 157.2, 154.4, 140.9, 134.8, 128.3, 126.2, 125.8 (2C), 124.5, 124.3, 123.9, 72.5, 53.6, 49.9, 37.3, 36.9, 27.9, 25.5; IR (film) ν_{max} 3283, 2938, 2857, 1672, 1621, 1591 cm^{-1}; FABHRMS (NBA−NaI) *m/z* 379.1081 (M^+, $C_{18}H_{21}NO_6S$ requires 379.1090).

***N*-(Methoxycarbonyl)-1,2,3,4,11,11a-hexahydrocyclopropa[*c*]naphtho[2,1−*b*]azepin-6-one (*N*-CO_2Me-CNA, 29).** Following the general procedure detailed for **10**, **27** (0.0071 g, 0.019 mmol, 1 equiv) was treated with DBU (0.008 mL, 0.057 mmol, 3 equiv). Flash chromatography (SiO_2, 1 × 7 cm, 50% EtOAc−hexane with 5% Et_3N) furnished **29** as a colorless oil (0.0048 g, 0.0052 g theoretical, 90%). Recrystallization from 10% EtOAc−hexane gave colorless plates suitable for X-ray analysis:[24] mp 259−261 °C ; ^{1}H NMR (500 MHz, acetone-d_6) δ 8.13 (dd, J = 8.0, 1.5 Hz, 1H), 7.63 (ddd, J = 8.5, 7.5, 1.5 Hz, 1H), 7.42 (ddd, J = 8.0, 7.2, 1.5 Hz, 1H), 7.20 (d, J = 8.5 Hz, 1H), 6.52 (s, 1H), 4.26−4.15 (m, 1H), 3.61 (s, 3H), 2.79−2.73 (m, 1H), 2.32−2.28 (m, 1H), 2.18−2.09 (m, 3H), 1.96−1.94 (m, 1H), 1.80−1.78 (m, 1H), 1.69−1.65 (m, 1H); ^{13}C NMR (125 MHz, acetone-d_6) δ 185.6, 155.2, 146.5 (2C), 133.6, 132.9, 129.7, 126.7, 126.5, 123.2, 53.1, 48.6, 39.8, 33.5, 26.8, 25.8, 25.5; IR (film) ν_{max} 3067, 2923, 2851, 1708, 1646, 1600, 1446 cm^{-1}; FABHRMS (NBA−NaI) *m/z* 284.1281 (M + H^+, $C_{17}H_{17}NO_3$ requires 284.1287).

7-(Benzyloxy)-5-[(5,6,7-trimethoxyindol-2-yl)carbonyl]-1-methylidene-1,2,3,4−tetrahydro-5*H*-naphtho[1,2−*b*]-azepine (22). A solution of **20** (0.142 g, 0.405 mmol, 1 equiv) in DMF (3 mL) was treated with [[3-(dimethylamino)propyl]-ethyl]carbodiimide hydrochloride (EDCI, 0.233 g, 1.22 mmol, 3 equiv) followed by 5,6,7-trimethoxyindole-2-carboxylic acid (0.122 g, 0.486 mmol, 1.2 equiv), and the reaction mixture was stirred at 25 °C for 4.5 h. The crude reaction mixture was diluted with EtOAc (4 mL) and extracted with H_2O (2 mL). The aqueous portion was extracted with EtOAc (2 × 1 mL). The combined organic portions were dried ($MgSO_4$), filtered, and concentrated. Radial chromatography (SiO_2, 2 mm plate, 50% EtOAc−hexane) furnished **22** (0.177 g, 0.222 g theoretical, 80%) as a pale yellow solid: mp 88−90 °C; ^{1}H NMR (500 MHz, $CDCl_3$) major rotamer δ 9.30 (s, 1H), 8.47−8.44 (m, 1H), 7.98−7.97 (m, 1H), 7.63−7.57 (m, 2H), 7.39−7.36 (m, 2H), 7.26−7.18 (m, 3H), 6.72 (s, 1H), 6.46 (s, 1H), 6.23−6.18 (m, 1H), 5.31−5.27 (m, 1H), 5.19−5.14 (m, 1H), 5.09−5.04 (m, 1H), 4.94−4.89 (m, 1H), 4.02 (s, 3H), 3.88 (s, 3H), 3.75 (s, 3H), 3.67−3.61 (m, 1H), 2.18−2.10 (m, 5H); ^{13}C NMR (125 MHz, $CDCl_3$) major rotamer δ 162.1, 154.5, 149.4, 144.3, 139.8, 138.6, 137.3, 136.5, 136.4, 136.3, 132.0, 129.5, 128.4 (2C), 127.9, 127.1 (2C), 126.9, 126.3, 125.7, 123.4, 122.9, 118.2, 107.3, 106.9, 97.8, 70.2, 61.4, 56.0, 54.7, 47.3, 34.7, 25.2, 22.9; IR (film) ν_{max} 3448, 3235, 3062, 2930, 1607, 1581, 1495 cm^{-1}; FABHRMS (NBA−CsI) *m/z* 681.1378 (M + Cs^+, $C_{34}H_{32}N_2O_5$ requires 681.1366).

7-(Benzyloxy)-1-(hydroxymethyl)-5-[(5,6,7-trimethoxyindol-2-yl)carbonyl]-1,2,3,4−tetrahydro-5*H*-naphtho[1,2−*b*]azepine (24). Following the general procedure detailed for **15**, **22** (0.200 g, 0.365 mmol, 1 equiv) was treated with BH_3•SMe_2 (0.110 mL, 10 M, 9 equiv), quenched with H_2O (0.44 mL), and oxidized with aqueous 2.5 M NaOH (0.44 mL, 1.10 mmol, 3 equiv) and 30% aqueous H_2O_2 (0.373 mL, 9 equiv). Radial chromatography (SiO_2, 2 mm plate, 70% EtOAc−hexane) provided **24** (0.107 g, 0.207 g theoretical, 52%) as an amber oil. Recrystallization from EtOAc gave a white microcrystalline solid: mp 178−180 °C with decomposition; ^{1}H NMR (500 MHz, $CDCl_3$) major rotamer δ 9.26 (s, 1H), 8.48 (d, J = 10.4 Hz, 1H), 8.28 (d, J = 10.8 Hz, 1H), 7.68−7.65 (m, 1H), 7.60−7.57 (m, 1H), 7.35−7.33 (m, 2H), 7.22−7.13 (m, 3H), 6.66 (s, 1H), 6.43 (s, 1H), 5.23−5.21 (m, 1H), 5.13−5.10 (m, 1H), 5.03−4.99 (m, 1H), 4.95−4.90 (m, 1H), 4.24−4.21 (m, 2H), 4.03 (s, 3H), 3.87 (s, 3H), 3.73 (s, 3H), 3.26−3.20 (m, 1H), 2.46−2.40 (m, 1H), 1.95−1.92 (m, 1H), 1.30−1.23 (m, 3H); ^{13}C NMR (125 MHz, $CDCl_3$) major rotamer δ 160.7, 153.9, 149.5, 140.0, 139.8, 138.6, 136.3, 134.3, 129.0, 128.4 (2C), 127.8, 127.7, 127.1 (2C), 126.2, 125.9, 125.6, 124.8, 123.7, 123.3, 123.2, 108.4, 107.6, 97.9, 70.6, 70.2, 61.4, 61.1, 56.1, 41.3, 38.8, 31.8, 17.3; IR (film) 3446, 3290, 3062, 2927, 1732, 1608, 1587 cm^{-1}; FABHRMS (NBA−CsI) *m/z* 699.1482 (M + Cs^+, $C_{34}H_{34}N_2O_6$ requires 699.1471).

A solution of **24** (0.025 g) in 50% *i*-PrOH-hexane was resolved on a semipreparative Diacel Chiracel OD column (10 μm, 2 × 25 cm) using 30% *i*-PrOH−hexane as eluent (8 mL/min). The effluent was monitored at 254 nm, and the enantiomers were eluted with retention times of 20.9 and 24.0 min, respectively (α = 1.15). The fractions were collected and concentrated to afford (+)-(1*R*)-**24** (t_R = 20.9 min, 0.0088 g) and *ent*-(−)-(1*S*)-**24** (t_R = 24 min, 0.0093 g) with a 72% recovery (>99.9% ee).

(+)-(1*R*)-**24**: $[\alpha]^{25}_D$ +58 (*c* 0.044, EtOAc).[38]

ent-(−)-(1*S*)-**24**: $[\alpha]^{25}_D$ −56 (*c* 0.047, EtOAc).

7-(Benzyloxy)-1-[((methanesulfonyl)oxy)methyl]-5-[(5,6,7-trimethoxyindol-2−yl)carbonyl]-1,2,3,4-tetrahydro-5*H*-naphtho[1,2−*b*]azepine (26). Following the general procedure detailed for **16**, **24** (0.040 g, 0.071 mmol, 1 equiv) was treated with Et_3N (0.049 mL, 0.354 mmol, 5 equiv) and

CH_3SO_2Cl (0.011 mL, 0.141 mmol, 2 equiv). Radial chromatography (SiO_2, 1 mm plate, 70% EtOAc−hexane) furnished **26** (0.034 g, 0.046 g theoretical, 75%) as a white solid: mp 175−177 °C with decomposition; ^{1}H NMR (500 MHz, $CDCl_3$) major rotamer δ 9.30 (s, 1H), 8.49 (dd, J = 8.0, 1.0 Hz, 1H), 8.25 (d, J = 9.0 Hz, 1H), 7.68 (ddd, J = 8.0, 6.5, 1.0 Hz 1H), 7.61−7.58 (m, 1H), 7.36−7.34 (m, 2H), 7.22−7.16 (m, 3H), 6.69 (s, 1H), 6.43 (s, 1H), 5.28 (d, J = 2.0 Hz, 1H), 5.27−5.26 (m, 1H), 5.14 (d, J = 11.5 Hz, 1H), 5.03−4.99 (m, 2H), 4.52−4.49 (m, 1H), 4.04 (s, 3H), 3.88 (s, 3H), 3.74 (s, 3H), 3.21−3.17 (m, 1H), 2.78 (s, 3H), 2.60−2.59 (m, 1H), 2.20−2.18 (m, 1H), 1.34−1.32 (m, 3H); ^{13}C NMR (125 MHz, $CDCl_3$) major rotamer δ 160.7, 154.0, 149.6, 140.1, 139.9, 138.6, 136.2, 133.8, 128.7, 128.4 (2C), 127.9, 127.8, 127.1 (2C), 125.9, 125.7, 125.1, 124.9, 123.5, 123.3, 123.2, 108.6, 107.4, 97.8, 79.9, 70.2, 61.4, 61.1, 56.0, 41.4, 38.4, 36.7, 30.5, 16.9; IR (film) ν_{max} 3453, 3299, 3001, 2929, 2827, 1608, 1588 cm^{-1}; FABHRMS (NBA−CsI) m/z 777.1267 (M + Cs$^+$, $C_{35}H_{36}N_2O_6$ requires 777.1247).

(+)-(1*R*)-**26**: $[\alpha]^{25}_D$ +26 (*c* 0.044, EtOAc).[38]

ent-(−)-(1*S*)-**26**: $[\alpha]^{25}_D$ −28 (*c* 0.042, EtOAc).

7-Hydroxy-1-[((methanesulfonyl)oxy)methyl]-5-[(5,6,7-trimethoxyindol-2-yl)carbonyl]-1,2,3,4-tetrahydro-5*H*-naphtho[1,2−*b*]azepine (28). Following the general procedure detailed for **17**, **26** (0.024 g, 0.037 mmol, 1 equiv) was treated 10% Pd−C (0.006 g, 0.15 equiv) followed by aqueous HCO_2NH_4 (0.165 mL, 25% w/v, 18 equiv). Filtration and concentration gave **28** as an analytically pure colorless oil in quantitative yield (0.020 g, 0.020 g theoretical): ^{1}H NMR (500 MHz, acetone-d_6) major rotamer δ 10.17 (s, 1H), 9.20 (s, 1H), 8.37−8.34 (m, 2H), 7.68−7.56 (m, 2H), 6.66 (s, 1H), 6.51 (s, 1H), 5.42 (s, 1H), 5.23−5.22 (m, 1H), 4.95−4.92 (m, 1H), 4.60−4.59 (m, 1H), 3.98 (s, 3H), 3.79 (s, 3H), 3.68 (s, 3H), 3.21−3.13 (m, 1H), 3.05 (s, 3H), 2.55−2.43 (m, 1H), 2.19−2.16 (m, 1H), 1.40−1.37 (m, 3H); ^{13}C NMR (125 MHz, acetone-d_6) major rotamer δ 161.1, 153.4, 150.8, 141.3, 141.1, 139.8, 135.1, 130.6, 128.3, 126.0, 125.8 (2C), 125.0, 124.6, 124.3, 123.8, 110.7, 108.8, 98.7, 81.6, 61.4, 61.3, 56.3, 41.8, 38.1, 37.5, 31.2, 17.4; IR (film) ν_{max} 3313, 2936, 2836, 1731, 1592, 1584 cm^{-1}; FABHRMS (NBA−CsI) m/z 687.0751 (M + Cs$^+$, $C_{28}H_{30}N_2O_8S$ requires 687.0774).

(+)-(1*R*)-**28**: $[\alpha]^{25}_D$ +143 (*c* 0.036, THF).[38]

ent-(−)-(1*S*)-**28**: $[\alpha]^{25}_D$ −147 (*c* 0.036, THF).

***N*-[(5,6,7-Trimethoxyindol-2-yl)carbonyl]-1,2,3,4,11,11a-hexahydrocyclopropa[*c*]naphtho[2,1−*b*]azepin-6-one (30, CNA-TMI).** Following the general procedure detailed for **10**, **28** (0.0054 g, 0.001 mmol, 1 equiv) was treated with DBU (0.004 mL, 0.030 mmol, 3 equiv). Flash chromatography (SiO_2, 1 × 7 cm, 50% EtOAc−hexane with 5% Et_3N) furnished **30** as a yellow solid (0.0022 g, 0.0046 g theoretical, 48%). Recrystallization from EtOAc gave yellow needles: mp 222−227 °C; ^{1}H NMR (CD_3CN, 400 MHz) major rotamer δ 9.67 (br s, 1H), 8.15 (dd, J = 7.8, 1.3 Hz, 1H), 7.65−7.61 (m, 1H), 7.49−7.31 (m, 1H), 7.32 (d, J = 8.1 Hz, 1H), 6.77 (s, 1H), 6.63 (s, 1H), 6.12 (s, 1H), 4.29 (ddd, J = 12.0, 6.3, 5.3 Hz, 1H), 3.99 (s, 3H), 3.83 (s, 3H), 3.76 (s, 3H), 3.37 (ddd, J = 13.0, 8.5, 7.0 Hz, 1H), 2.86−2.83 (m, 1H), 2.54−2.48 (m, 1H), 2.32−2.27 (m, 2H), 1.31−1.26 (m, 3H); IR (film) ν_{max} 3292, 2923, 2841, 1626, 1600, 1523, 1456 cm^{-1}; FABHRMS (NBA−CsI) m/z 459.1934 (M + H$^+$, $C_{27}H_{26}N_2O_5$ requires 459.1920).

(−)-**30**: $[\alpha]^{25}_D$ −146 (*c* 0.004, THF).[38]

ent-(+)-**30**: $[\alpha]^{25}_D$ +146 (*c* 0.004, THF).

Acid-Catalyzed Addition of H_2O to 10: 6-(*tert*-Butyloxycarbonyl)-2,8-dihydroxy-1,2,3,4,5-pentahydro-6*H*-naphtho[1,2−*b*]azocine (31). A solution of **10** (0.0074 g, 0.022 mmol, 1 equiv) in THF (0.75 mL) was treated with H_2O (0.25 mL) followed by CF_3SO_3H (0.027 mL, 0.1 M in THF, 0.12 equiv) at 25 °C, and the mixture was stirred for 5 min. The reaction mixture was treated with $NaHCO_3$ (0.01 g) followed by H_2O (1.0 mL). The aqueous portion was extracted with EtOAc (2 × 1 mL), and the combined organic portions were dried ($MgSO_4$), filtered, and concentrated to a colorless oil. ^{1}H NMR analysis of the crude mixture and comparison with **33** indicated the presence of the ring expansion solvolysis product exclusively (≥40−20:1). Radial chromatography (SiO_2, 1 mm plate, 50% EtOAc−hexane) provided **31** as a colorless oil (0.0077 g, 0.0078 g theoretical, 99%) which slowly crystallized upon storage: mp 235−237 °C; ^{1}H NMR (400 MHz, acetone-d_6) major rotamer δ 9.08 (s, 1H), 8.26 (d, J = 8.3 Hz, 1H), 8.11 (d, J = 8.5 Hz, 1H), 7.57−7.54 (m, 1H), 7.49−7.44 (m, 1H), 6.68 (s, 1H), 4.38−4.35 (m, 1H), 4.07−3.95 (m, 1H), 3.40−3.35 (m, 1H), 3.02−2.80 (m, 2H), 2.01−1.93 (m, 1H), 1.71−1.63 (m, 1H), 1.52−1.44 (m, 1H), 1.28 (s, 9H), 1.20−1.17 (m, 2H); IR (film) ν_{max} 3309, 2977, 2927, 2867, 1689, 1664, 1619, 1589 cm^{-1}; FABHRMS (NBA−CsI) m/z 476.0848 (M + Cs$^+$, $C_{20}H_{25}NO_4$ requires 476.0838).

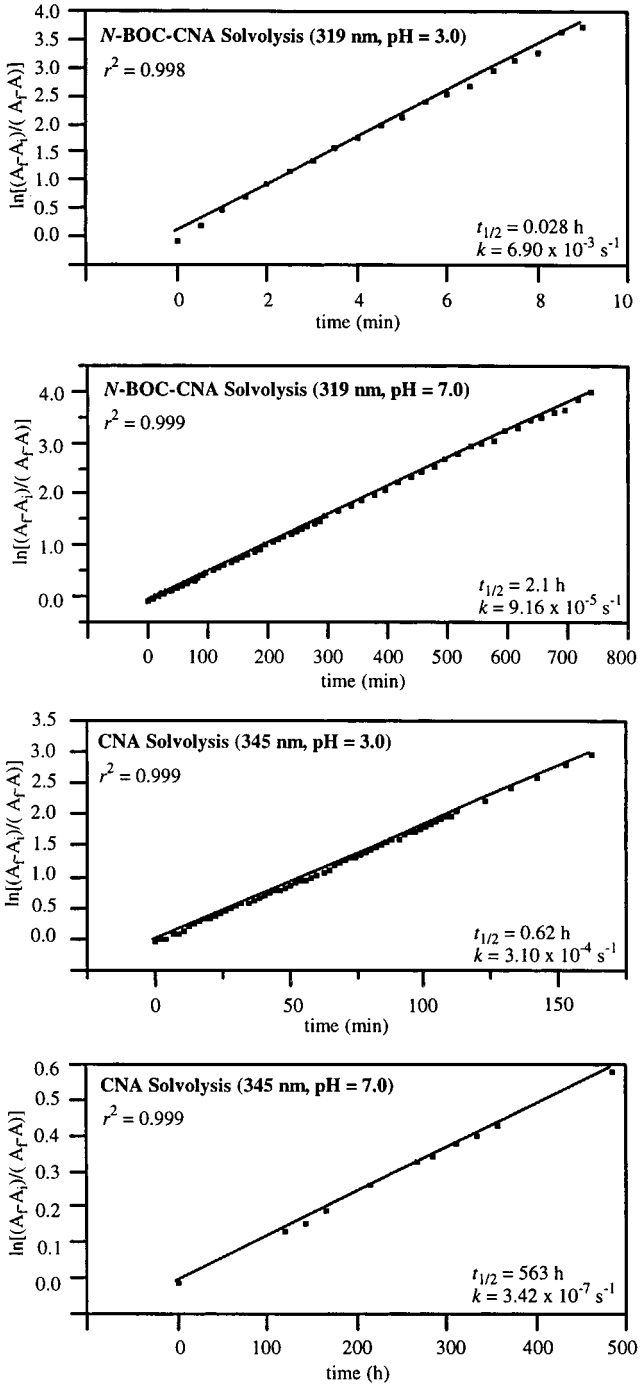

Figure 11.

Acid-Catalyzed Addition of H_2O to (+)-10: (−)-6-(*tert*-Butyloxycarbonyl)-2,8-dihydroxy-1,2,3,4,5-pentahydro-6*H*-naphtho[1,2−*b*]azocine (31). A solution of (+)-**10** (0.0030 g, 0.009 mmol, 1 equiv) in THF (0.38 mL) was treated with H_2O (0.13 mL) followed by CF_3SO_3H (0.011 mL, 0.1 M in THF, 0.12 equiv) at 25 °C, and the mixture was stirred for 5 min. Workup as described for racemic **31** and radial chromatography (SiO_2, 1 mm plate, 50% EtOAc−hexane) provided (−)-**31** as a colorless oil (0.0032 g, 0.0032 g theoretical, 99%) which slowly crystallized upon storage. This material was identical

with racemic **31** in all respects. The solvolysis of (+)-**10** provided a single enantiomer (Figure 4) established by chiral phase HPLC separation on a ChiralCel OG column (10 μm, 0.46 × 25 cm, 5% *i*-PrOH-hexane, 1 mL/min).

(−)-(2*R*)-**31**: $[\alpha]^{25}_{D}$ −9 (*c* 0.009, THF).

5-(*tert*-Butyloxycarbonyl)-7-hydroxy-1-(hydroxymethyl)-1,2,3,4-tetrahydro-5*H*-naphtho[1,2−*b*]azepine (33). Following the general procedure detailed for **17**, **15** (0.015 g, 0.035 mmol, 1 equiv) was treated with 10% Pd−C (0.001 g, 0.3 equiv) followed by aqueous HCO_2NH_4 (0.2 mL, 25% w/v, 23 equiv). Filtration and concentration gave **33** as an analytically pure colorless oil in quantitative yield (0.012 g, 0.012 g theoretical) which crystallized upon storage: mp 202−203 °C; ^{1}H NMR (400 MHz, $CDCl_3$) major rotamer δ 9.19 (s, 1H), 8.07−8.05 (m, 1H), 7.26−7.22 (m, 1H), 6.81−6.75 (m, 2H), 6.50 (s, 1H), 4.28−4.24 (m, 1H), 4.18−4.08 (m, 2H), 3.89−3.86 (m, 1H), 2.85−2.79 (m, 1H), 2.11−2.07 (m, 1H), 1.94−1.91 (m, 1H), 1.70−1.67 (m, 2H), 1.62 (s, 9H); ^{1}H NMR (400 MHz, acetone-d_6) major rotamer 9.03 (s, 1H), 8.26 (d, J = 8.2 Hz, 1H), 8.07 (d, J = 8.6 Hz, 1H), 7.55−7.51 (m, 1H), 7.46−7.43 (m, 1H), 6.74 (s, 1H), 4.37−4.33 (m, 1H), 4.03−3.99 (m, 1H), 3.91−3.80 (m, 1H), 3.61−3.52 (m, 2H), 2.73−2.66 (m, 1H), 2.36−2.32 (m, 1H), 2.20−2.10 (m, 1H), 1.60−1.55 (m, 1H), 1.33 (s, 9H); IR (film) ν_{max} 3272, 2976, 2925, 1662, 1621, 1596 cm^{-1}; FABHRMS (NBA−NaI) *m*/*z* 344.1855 (M + H$^+$, $C_{20}H_{25}NO_4$ requires 344.1862).

Acid-Catalyzed Addition of CH_3OH to 10: 6-(*tert*-Butyloxycarbonyl)-8-hydroxy-2−methoxy-1,2,3,4,5-pentahydro-6*H*-naphtho[1,2−*b*]azocine (32). A solution of **10** (0.0069 g, 0.021 mmol, 1 equiv) in freshly distilled CH_3OH (1.0 mL) was treated with CF_3SO_3H (0.027 mL, 0.1 M in CH_3OH, 0.12 equiv) at 25 °C for 5 min. Workup as described for **31** and radial chromatography (SiO_2, 1 mm plate, 50% EtOAc−hexane) provided **32** as a colorless oil (0.0070 g, 0.0076 g theoretical, 92%) which slowly crystallized upon storage: mp 199−200 °C with decomposition; ^{1}H NMR (500 MHz, acetone-d_6) major rotamer δ 9.09 (s, 1H), 8.27 (d, J = 8.5 Hz, 1H), 8.11 (d, J = 8.5 Hz, 1H), 7.59−7.56 (m, 1H), 7.49−7.47 (m, 1H), 6.69 (s, 1H), 4.37−4.29 (m, 1H), 3.57−3.56 (m, 1H), 3.49−3.46 (m, 1H), 3.43 (s, 3H), 2.85−2.79 (m, 2H), 1.99−1.90 (m, 1H), 1.81−1.75 (m, 1H), 1.28 (s, 9H overlapping with m, 2H); IR (film) ν_{max} 3268, 2971, 2868, 1695, 1664, 1587 cm^{-1}; FABHRMS (NBA−CsI) *m*/*z* 357.1951 (M + Cs$^+$, $C_{21}H_{27}NO_4$ requires 357.1940).

Addition of HCl to 10: 6-(*tert*-Butyloxycarbonyl)-2-chloro-8-hydroxy-1,2,3,4,5−pentahydro-6*H*-naphthol[1,2−*b*]azocine (34). A solution of **10** (0.0031 g, 0.0095 mmol, 1 equiv) in THF (0.31 mL) was treated with 3.3 M HCl−THF (0.0043 mL, 1.5 equiv) at −78 °C for 5 min. Evaporation of the volatiles and chromatography (SiO_2 1 × 7 cm, 30% EtOAc−hexane) furnished **34** as a pure white foam (0.0034 g, 0.0034 g theoretical, 100%): ^{1}H NMR (400 MHz, acetone-d_6) major rotamer δ 9.27 (br s, 1H), 8.27 (d, J = 8.5 Hz, 1H), 8.06 (d, J = 8.5 Hz, 1H), 7.63−7.59 (m, 1H), 7.57−7.49 (m, 1H), 6.72 (s, 1H), 4.49−4.43 (m, 1H), 3.67−3.63 (m, 1H), 3.24−3.21 (m, 1H), 2.88−2.82 (m, 2H), 2.02−1.90 (m, 1H), 1.81−1.75 (m, 1H), 1.68−1.67 (m, 1H), 1.43−1.41 (m, 1H), 1.29 (s, 9H); IR (film) ν_{max} 3251, 2974, 2933, 1692, 1662, 1621, 1585 cm^{-1}; FABHRMS (NBA−NaI) *m*/*z* 384.1333 (M + Na$^+$, $C_{20}H_{24}ClNO_3$ requires 384.1342).

Aqueous Solvolysis of *N*-BOC-CNA (10) and CNA (11). Samples of **10** (150 μg) and **11** (150 μg) were dissolved in CH_3OH (1.5 mL), and the resulting solutions were mixed with aqueous buffer (pH 3, 1.5 mL, 4:1:20 (v:v:v) 0.1 M citric acid, 0.2 M Na_2HPO_4, and deionized H_2O, respectively). Similarly, samples of **10** (150 μg) and **11** (150 μg) in CH_3OH (1.5 mL) were mixed with deionized H_2O (pH 7, 1.5 mL). The UV spectra of the solutions were measured immediately after mixing with the appropriate aqueous solution. The blank and the solvolysis reaction solutions were stoppered, protected from light, and allowed to stand at 25 °C. The total reaction times reflect those required to observe no further change in absorbance. For the solvolysis of **10** at pH 3, the UV spectrum was taken every 30 s for 10 min and then every 3 min for the next 40 min. The decrease of the absorbance at 319 nm was monitored. The solvolysis rate was calculated from the least squares treatment (r^2 = 0.998) of the slope of a plot of time versus $\ln[(A_f - A_i)/(A_f - A)]$ (Figure 11); $k = 6.90 \times 10^{-3}$ s^{-1}, $t_{1/2}$ = 1.7 min, 0.028 h. For the solvolysis of **10** at pH 7, the UV spectrum was monitored every 5 min for 19 h. The rate was calculated from the least squares treatment of the same type of plot as above (r^2 = 0.999); $k = 9.16 \times 10^{-5}$ s^{-1}, $t_{1/2}$ = 126 min, 2.1 h. For the solvolysis of **11** at pH 3, the UV spectrum was monitored every 2 min for the first 110 min and then every 10 min for the next 4 h. The decrease in the absorbance at 345 nm was recorded. The solvolysis rate constant was calculated from the least squares treatment of the same type of plot as above (r^2 = 0.999); $k = 3.10 \times 10^{-4}$ s^{-1}, $t_{1/2}$ = 37 min, 0.62 h. For the solvolysis of **11** at pH 7, the UV spectrum was taken every 24 h for 21 d. The rate was calculated from the least squares treatment of the same type of plot as above (r^2 = 0.999); $k = 3.42 \times 10^{-7}$ s^{-1}, $t_{1/2}$ = 563 h.

Acknowledgment. We gratefully acknowledge the financial support of the National Institutes of Health (CA55276) and the Skaggs Institute for Chemical Biology. We thank Dr. P. Mésini and N.-E. Haynes for preliminary studies (eq 2), Dr. Raj K. Chadha for the X-ray structure determinations, and Dr. Qing Jin for the in vitro cytotoxicity evaluations summarized in Table 4.

Supporting Information Available: Full experimental details for the preparation of substrates found in eqs 1 and 2, summary tables of the data employed in Figure 10, and ^{1}H NMR spectra of **10**, **11**, **13**−**33** (31 pages). This material is contained in libraries on microfiche, immediately follows this article in the microfilm version of the journal, and can be ordered from the ACS; see any current masthead page for ordering information.

JO9707085